International Journal of Disaster Risk Reduction 95 (2023) 103903

Contents lists available at ScienceDirect

International Journal of Disaster Risk Reduction

journal homepage: www.elsevier.com/locate/ijdrr

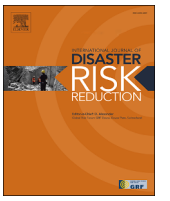

An archetype-based automated procedure to derive global-local seismic fragility of masonry building aggregates: META-FORMA-XL

Sergio Ruggieri [a], Francesco Salvatore Liguori [b], Valeria Leggieri [c], Antonio Bilotta [b], Antonio Madeo [b], Siro Casolo [d], Giuseppina Uva [a, *]

[a] DICATECH Department, Polytechnic University of Bari, Via Orabona 4, Bari, Italy
[b] DIMES Department, University of Calabria, Via P. Bucci 42/C, Rende, Italy
[c] SAAD Department, University of Camerino, Viale della Rimembranza 3, Ascoli Piceno, Italy
[d] ABC Department, Polytechnic University of Milan, Via Giuseppe Ponzio, 31, Milano, Italy

ARTICLE INFO

Keywords:
Seismic fragility
Historical centres
Masonry aggregates
Local collapse mechanisms
Global collapse mechanisms

ABSTRACT

The paper presents an automated procedure for deriving fragility curves for typological masonry aggregates, named META-FORMA-XL (MEchanical-Typological Approach FOR Masonry Aggregates – X Local). The topic deals with the urban-scale seismic vulnerability analysis, which can provide powerful information for developing risk mitigation plans and implementing strategies for reducing expected losses. However, when masonry buildings in aggregate are analysed, many issues arise, related to the lack of data, the complexity of the structural configurations and the presence of uncertainties. To this scope, the proposed procedure aims to investigate the seismic behaviour of masonry aggregates, based on numerical analyses carried out on ideal representations of the existing building stock, indicated as archetypes, by modelling geometrical and mechanical uncertainties characterizing buildings in the studied area. The archetype buildings are made according to exposure analyses by combining typical inventory collection forms and information derived from freely available databases. By investigating the seismic response of numerical models for a high number of archetype buildings, fragility curves are derived for all limit-states and two main directions, accounting for global and local damage mechanisms. The procedure is tested on low-rise row masonry aggregates in Southern Italy. The output of the procedure is validated on a real case study, for which a near-full information on the geometrical and mechanical features is available, providing a critical comparison in terms of fragility curves. Results highlight several advantages of the proposed approach, such as the possibility of identifying the most likely collapse mechanism for a specific masonry aggregation, the simplicity and the celerity of the analyses despite the large number of archetype models, and the exhaustive consideration of the uncertainties. Finally, the proposed concept can be readily extended to other aggregation forms and structural typologies.

1. Introduction

The disastrous effects of the recent seismic events on the Mediterranean area, as occurred after the 2023 Turkey-Syria Earthquake, have highlighted once again the issue of the high vulnerability of the existing building stock, which in many cases presents characteristics not adequate to face unpredictable hazardous events. The observed high and often intangible losses have raised the urgent ne-

* Corresponding author.
E-mail address: giuseppina.uva@poliba.it (G. Uva).

https://doi.org/10.1016/j.ijdrr.2023.103903
Received 1 June 2023; Received in revised form 27 July 2023; Accepted 28 July 2023
Available online 30 July 2023

cessity to develop adequate risk mitigation plans for existing buildings, able to predict the effects of seismic events and to reduce the expected losses, e.g., human deaths, economic damages, service interruptions, by employing adequate prevention measures. With this goal in mind, over the last 20 years, several methodologies were developed to quantify the vulnerability of the existing building stock (or of a part of it), providing reliable tools to mitigate the seismic risk. As a first classification, two main alternatives can be mentioned: (a) empirical methods; (b) mechanical methods. Empirical methods consist in the statistical processing of data aimed at calibrating and estimating the vulnerability of classes of buildings. In this case, input data are represented by the observations of real damages occurred after past earthquakes. Generically, the output is represented by curves reporting the probability of occurrence of a certain damage state for increasing seismic intensities, quantified in terms of instrumented (e.g., peak ground acceleration, PGA) or not instrumented (e.g., macroseismic scales, as the Mercalli-Cancani-Sieberg) intensity measures (IMs). Several examples are offered by the scientific literature, about reinforced concrete (RC) [1] and masonry [2] buildings, as the most common in the urban environment. Mechanical methods consist in the definition of representative numerical models, which can be investigated and analysed to derive the vulnerability of classes of buildings. In this case, the outcome of the investigation depends on the proposed simulation, which is related to the type and accuracy of the modelling and to the analysis steps. It is worth noting that, regarding the numerical models, different options can be employed, by exploiting few real buildings representative of a class (i.e., index buildings), or by opting for ideal models characterized by the structural features of the existing building stock (i.e., archetype buildings). In both cases, the output is represented by fragility curves, representing the probability of exceeding a certain physical state of the structure (quantified through a specific engineering demand parameter, EDP), for increasing seismic intensities. Examples of mechanical methods are available for RC [3] and masonry [4] buildings, exploiting simple or complex models, static or dynamic analyses [5]. Straddling empirical and mechanical methods, other methodologies for large-scale analysis could be mentioned, among which the rapid visual screening methods, which consist in the collection of typological data from *ad hoc* questionnaires and the processing of information to provide a synthetic index, useful to derive a prioritization scale among buildings in the focused area [6], and the hybrid methods, which combine post-earthquake damages and mechanical models to improve the vulnerability function [7].

Regardless of the employed approach, the reliability of the prediction depends on two main parameters and their interconnection: (i) the size of the focused area; (ii) the data at disposal. Concerning the first point, if a large area is analysed, buildings with different features need to be considered. This means that specific taxonomies with few parameters must be elaborated (e.g., year of construction, structural typologies, number of storeys) under which clustering the buildings. If the area under consideration reduces, taxonomies can be better characterised, and the accurateness of the prediction improved. Several examples of taxonomies exist, from the initial [8,9] to the recently developed ones [10]. Regarding to the data at disposal, the accuracy of the vulnerability function depends on the quality and the quantity of information to process. For example, opting for a mechanical method based on archetype buildings, a detailed 3D model can be arranged only if a near-full characterization of mechanical and geometrical features is available. Instead, if few parameters are known, only simple models can be employed (e.g., single-degree-of-freedom). Thus, to collect useful data for vulnerability analysis purpose, different sources can be considered, starting from the simple census data (containing the number of floors, construction material and year of construction), up to the available freely georeferenced databases, such as the cadastral maps (reporting the contours of buildings) and the technical regional cartographies (containing information on buildings within a polygon, as the area and the height). To consistently improve the quality and quantity of data, it is necessary resorting interviews-based methods, which allow to collect data through predefined survey forms characterized by all features to be used in a seismic vulnerability analysis. Considering the country of the authors of the paper, the main option is represented by CARTIS [11], adequate to collect information at urban scale. This latter consists in a form containing typological information, subdivided in specific fields, on which the surveyor can select the likely options from multiple-choice lists. The data do not regard a specific building, but a sample of buildings characterized by the same typological features and that fall into the so-called homogeneous town compartments (TCs). In general, the CARTIS survey is compiled after interviewing some local experts (e.g., old practitioners), which present a deep know-how and a historical view about the building stock evolution along the territory. After, the data at disposal for each homogeneous TC are processed (usually, data are implemented in GIS environment and integrated with layers containing other information) and used to develop vulnerability functions. Several examples of CARTIS-based methodologies are available in the scientific literature, among which the mechanical [12–14] or vulnerability index approaches [15].

Within this complex framework of large-scale methodologies and although the existence of several options to develop risk mitigation plans, the matter becomes more intricated when coming to historical centres. With this regard, manifold aspects should be considered, which lead to shift the current paradigms in large-scale analysis of the existing buildings stock. First, buildings in historical centres are disposed in a complex fabric, as result of human expansions and superfetation actions over the years. After, in most of the cases, historical centres present a disposition of buildings in clusters, and then, from the structural point of view, the aggregation of structures shall be considered to effectively predict the seismic behaviour. Finally, the presence of a high variety of constructive materials and techniques (also within the same building) provides an elevated uncertainty degree, which resides in both geometrical and mechanical features and that can limit the reliability of the vulnerability analysis prediction. Near to these aspects, it is worth noting that several obstacles emerge in the application of empirical and mechanical methods. As a matter of fact, the application of empirical methods to buildings in aggregate is not an option to account for, because all forms developed in the past for collecting observed damages are referred to single buildings, in which the aggregation is usually considered as an additional parameter (e.g., the building is isolated or not isolated). On the other hand, also mechanical methods for masonry aggregates still represent an open issue, considering the necessity to combine an effective model selection (i.e., an index or an archetype building, as representative of a part of the building stock within the focused historical centre), a right modelling approach (that accounts for the possible failure mechanisms and structural interactions), and an elevated uncertainty in the involved parameters (that can require a high-consuming effort in the modelling and analysis phases).

Thus, on the base of the above reported information, there is the necessity to develop a procedure tailored for masonry aggregates in historical centres and aimed at evaluating their seismic vulnerability at large-scale. With this goal in mind, this paper proposes META-FORMA-XL, acronym of MEchanical-Typological Approach FOR Masonry Aggregates – X Local, which combines the information obtained by interview-based approaches with a mechanical method developed on the concept of archetype buildings. In detail, the first phase of the procedure consists in an exposure analysis of the area under investigation, by collecting information from different sources, i.e., freely available databases and the output of the CARTIS form. After, the available data are organized in a simple taxonomy, which differentiates deterministic from uncertain parameters. This data organization allows to build specific archetype buildings, as mechanical models characterized by the identified deterministic parameters, and on which vary uncertain parameters in plausible ranges through an automated procedure of model generation that exploits the direct interaction between the programming software MATLAB [16] and the structural analysis and design software POR2000 [17]. At this point, a large set of numerical models is generated and can be investigated under seismic actions with regard to global and local failure mechanisms. As output of the procedure, fragility curves can be computed, accounting for different failure modes (i.e., local and global), different analysis directions, and different limit-states. The proposed procedure was tested on the data available for the historical centre of Foggia, Southern Italy, which is characterized by different types of row masonry aggregates. The reliability of the obtained results was also evaluated towards a real case study, for which a near-full knowledge of the geometrical and mechanical parameters was available. META-FORMA-XL represents the upgrade of the first version of the procedure, named META-FORMA and developed in Ref. [4]. Unlike META-FORMA, which provided a detailed description on how automatize the process of generation and analysis of masonry aggregates, the main novelty aspects of META-FORMA-XL are: (a) a specific methodology for selecting the useful parameters and values for performing a probabilistic-based large-scale analysis of masonry aggregates in historical centres; (b) the estimate of global fragility curves for each direction and limit-state, (b) the estimate of local fragility curves for each direction and limit-state. At the same time, although different output from Ref. [4] are provided (from META-FORMA, bilinear curves and capacity/demand ratios for all limit-states were derived), the proposed procedure does not lose the strengths of the original procedure, i.e., the evaluation of the interaction among structural units, the fully automation of model and analysis phases, and the required low computational effort.

2. Background

The behaviour of masonry aggregates is still an open issue in the recent scientific literature, considering that the focus has been often devoted to the study of single masonry buildings and their behaviour under static and seismic loads. In this field, a myriad of studies could be mentioned, which investigate the behaviour of masonry buildings through analytical (e.g., Ref. [18]), experimental (e.g., Ref. [19]), and numerical (e.g., Ref. [20]) analyses. When coming to the seismic behaviour of buildings in historical centres, the investigation of single structural units could be not representative of the real behaviour, considering that the interaction with other buildings could heavily modify the result. For this reason, this section reports an overview about the studies related to the seismic behaviour of masonry aggregates. From the modelling point of view, the aggregation effect on the focused building could be investigated in two alternative ways.

- Investigation of the single buildings and identification of the boundary conditions to be applied for accounting the interaction with the contiguous structural units (e.g., by adding external forces).
- Investigation of the entire aggregate system, considering all structural units (or portions) interacting with the focused building.

Looking at the seismic behaviour, the aggregation effect implies a modification in terms of mass (under seismic excitation, the contiguous buildings represent additional masses) and stiffness (under seismic excitation, the contiguous buildings represent additional restraints) on the focused structural unit, which can severely modify local and global behaviour. According to the existing literature, one of the first studies is proposed in Ref. [21], in which authors investigated the influence of the aggregation effect on the overturning mechanisms of a single structural unit. To this scope, authors employed different finite element (FE) models and accounted for the mechanical nonlinearities of the masonry. The obtained results showed how the aggregation effect influenced the flexibility and the safety factor of the focused building, outlining the so-called *group effect* provided by the aggregation. In Ref. [22], authors investigated row masonry aggregates by focusing on the aggregation length and on the effect of slab flexibility, by employing a macro-modelling approach and nonlinear dynamic analyses. Authors explored the seismic behaviour of different aggregate configurations for one-room and two-rooms cells, highlighting the differences at the variation of the aggregation shapes. In Ref. [23], authors proposed two numerical models as representative of the masonry buildings in the Azores, accounting for only in-plane mechanisms. The results in terms of nonlinear static analysis highlighted how the aggregation configuration influenced the global seismic response, focusing also on the global behaviour of the adjacent buildings (local failures were neglected). In Ref. [24], authors investigated two historical masonry aggregates with complex shape, by means of a nonlinear FE model. From the investigation, authors outlined that the aggregation leads to the high vulnerability for the perimeter walls, which suffered of large displacements due to the presence of openings. In addition, authors showed that the seismic vulnerability increase due to the inefficient connection among structural units and in presence of torsional effects. In Ref. [25], authors investigated the global behaviour of a masonry aggregate in Portugal. In particular, the so-called *target structural unit* approach was proposed, which aimed at identifying the required part of adjacent buildings to consider for accounting the aggregation effect on the focused building, by gradually varying the boundary conditions and investigating the seismic behaviour through nonlinear static analysis. Results showed that the selection of the optimal part of aggregate depends on the structural features of the adjacent buildings, such as the geometrical and mechanical properties. In Refs. [26,27], authors proposed ANUB-Aggregates, in which, by exploiting the NURBS approach [28], the quantification of local failures in masonry aggregates was investigated. In detail, by using an adaptive upper bound limit-analysis, the most likely local failure mechanisms were

identified in masonry aggregates, also accounting for peculiar elements in historical buildings, such as arches or vaults. Recently, in Ref. [29], authors estimated fragility curves for a masonry aggregate with L-shape with three structural units, modelled through a macro-element approach and analysed through nonlinear dynamic analyses. As results, in addition to provide fragility curves for in-plane and out-of-plane mechanisms, some insights were offered about the corner structural unit as the main focused building and about the differences obtained from different types of connections among structural units. In Ref. [30], a procedure was proposed to investigate the pounding effect among buildings in a masonry aggregates, accounting for local and global mechanisms and looking at the influence of different soil conditions. As output, authors showed that the site effects can strongly affect the seismic vulnerability of the cluster, by modifying the occurrence of in-plane and out-of-plane mechanisms. Near to the numerical investigations above reported, in the recent years some studies focused on the seismic behaviour of masonry aggregate effects through experimental tests. In Ref. [31], a unidirectional shake-table test was performed on a half-scale prototype of stone masonry building aggregate. The specimen was arranged through two weakly connected structural units with three-storey height and timber floor. The results of the test showed the inelastic behaviour of the cluster, with the occurrence of in-plane and out-of-plane mechanisms and two main achievements: a permanent elongation of the spandrels and a separation between the two structural units in the upper part. Combining experimental tests and different modelling approaches, in Ref. [32] several research groups exploited data provided by a shake-table test of a two-unit, double-leaf stone masonry aggregate subjected to two horizontal components of dynamic excitation, to provide numerical results within a blind prediction. Different insights were provided, showing the capacity of each modelling approach to predict local and global mechanisms.

Although the above state-of-the-art is referred to specific cases and generalized to the main issues characterizing the seismic analysis of masonry aggregates, most of the procedures developed are not adequate for a large-scale analysis, considering that the investigation of a specific case could be not representative of the overall situation in a historical centre, and it can be also extremely time-consuming. Hence, slim approaches are recommended, able to account for the uncertainty while adopting adequate simplifications. With this regard, in Ref. [33] a simple method based on the Italian Guidelines on Cultural Heritage [34] was applied on two different masonry aggregates, and it was compared with numerical results provided by FE modelling simulation. Results showed that the proposed simplified procedure provided similar results in terms of base shear to the ones obtained by numerical model, even if slightly conservative. In Ref. [35] a hybrid method was proposed, which correlated the results of nonlinear static analysis and the macroseismic methodology [36]. Results were later compared with two indirect methods, proposing different vulnerability indexes. The application of the methodologies on some case studies revealed that the index methods provide higher vulnerability than the one obtained from the hybrid approach, but they are to prefer where the knowledge level is poor. In Ref. [37], authors proposed a vulnerability index to be applied for the seismic analysis at large-scale of masonry aggregates. The method consisted in a new survey form (based on existing interview-based methods), which accounted for some specific parameters to evaluate when facing masonry aggregates, such as the position of the focused building and the interaction between adjacent structural units. The results were validated with numerical models and tested on real case studies (the same approach was used in Ref. [38]). In Ref. [39], authors proposed a comparison among mechanical (Vulnus method was used [40]) and empirical approaches to investigate the seismic vulnerability of masonry aggregates and the single buildings composing the cluster. Results of analyses showed that the mechanical approaches provide more refined prediction of damages than empirically based ones. In Ref. [41], a simplified procedure was proposed to investigate historical aggregates in Sicily, Italy, based on a near-full typological analysis, and the investigation of representative aggregates through nonlinear static analysis. Results were given with reference to a particular aggregate configuration and some insights were provided about the structural interaction among buildings. In Ref. [42], authors adopted two different methodologies to derive the vulnerability of masonry aggregates in the historical centre of Campotosto, on the base of the empirical results in Ref. [43] and the results provided by Vulnus method [40]. The results were expressed in terms of fragility curves and the two output were compared in order to assess pros and cons of the two methods. In Ref. [44], authors proposed a new index-based procedure to investigate seismic vulnerability of masonry aggregates. In detail, the index was defined by weighing observational parameters (to which a score was assigned) and accounting for the quality of the masonry. Finally, authors showed the application of the index on the masonry aggregates of the Castelpoto historical centre, Southern Italy, showing the index variability by employing different earthquake scenarios. Finally, we close this state-of-the-art presentation by mentioning the automated mechanical method named META-FORMA [4], a procedure to estimate the global seismic vulnerability of masonry aggregates at large-scale. In particular, the approach exploited the information related to a single building belonging to an existing masonry aggregate (i.e., multi-source data derived from existing GIS databases and CARTIS data), to automatically generate typologically defined masonry aggregates through the programming software MATLAB [16] and the structural analysis and design software POR2000 [17]. Models were analysed through nonlinear static analyses and the output consisted in the capacity/demand ratios, which provided a rational result in the evaluation of the seismic vulnerability of masonry aggregates. This represents the starting point of the proposed procedure, which is comprehensively described in Section 3.

3. Meta-forma-xl: archetype-based seismic fragility of masonry aggregates

The framework of META-FORMA-XL is reported in Fig. 1, and it is composed by 6 steps, which are described in the following Subsections. To summarize the following contents, META-FORMA-XL can be subdivided in six steps: (1) data collection of information about the existing building stock, by using interview-based approaches or freely available databases; (2) feature selection, subdividing data among deterministic and uncertain parameters; (3) automated generation of archetype models, accounting for uncertainties of the selected parameters; (4) global analysis of archetype models; (5) local analysis of archetype models; (6) derivation of fragility curves for both local and global mechanisms with respect to each limit-state and each analysis direction. On this basis, the main advantages of the proposed approach can be here anticipated: (a) identification of the most likely collapse mechanisms in the studied

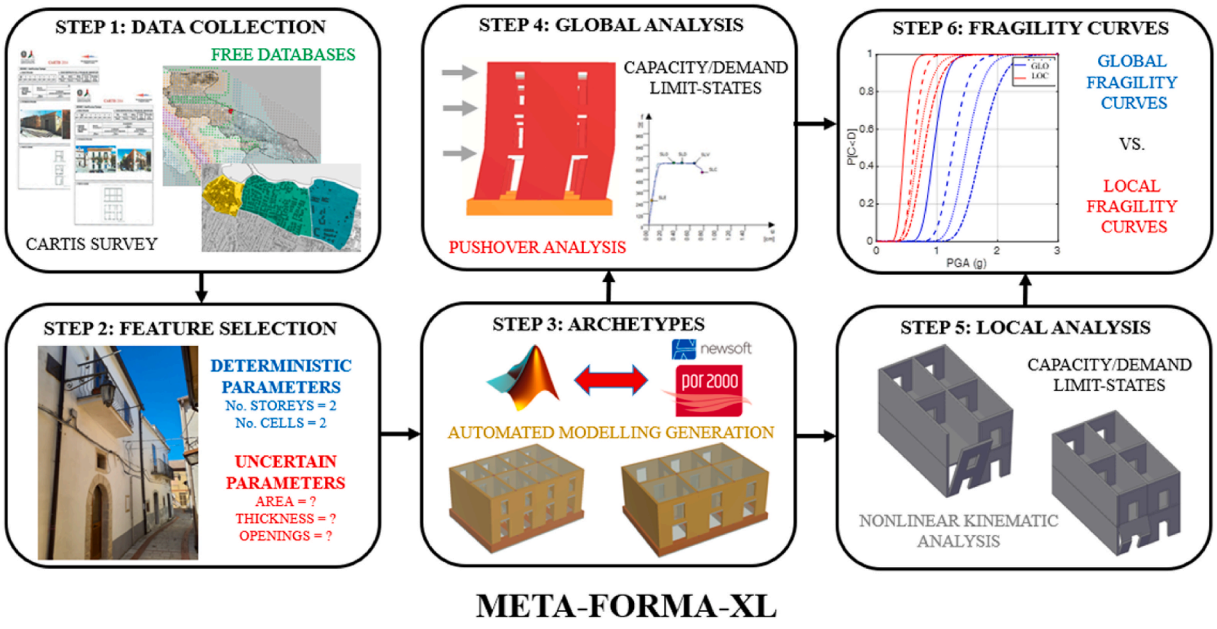

Fig. 1. Framework of META-FORMA-XL

masonry aggregates by using the tool of fragility curves; (b) possibility to perform seismic large-scale analysis of masonry aggregates in historical centres with a moderate computational effort; (c) consideration of all possible sources of uncertainty (i.e., geometrical, and mechanical features) in a view of probabilistic-based analysis.

3.1. Data collection

The first step of the proposed procedure consists in the data collection of the building stock in the area under investigation. Different sources can be exploited, with the aim to integrate information at the base of the investigation. The main source to draw from is the output of the CARTIS survey, which represents the minimum requirement to develop the proposed procedure. As above stated, the database from CARTIS contains structural typological information for buildings in TCs, among which base area, construction typology, foundation type, year of construction, interstorey height, number of windows per storey, presence or not of non-structural elements.

It worth remembering that data extracted from CARTIS database is reported within some predefined ranges, and then there is not a specific value to consider for each typological parameter. Close to the CARTIS data, the overall starting information can be enriched by employing data from freely available databases. Among the most common ones (taking as reference Italy and on the base of the authors' knowledge), it is worth retrieving the Census database, the cadastral maps, and the technical regional cartographies. Although the specific contribute provided by each above database is explicated in the Introduction, it is worth specifying that data can be overlapped and integrated, with the aim to better characterize each structural unit in the focused area. At the same time, regarding the main topic of the paper, the information about the aggregation is missing in all above sources, because data are always referred to single buildings. Hence, the best way to define the aggregation is the management of the databases in a GIS environment, in order to display data as layers and to identify the clustering typologies in the focused area. In the end, it is possible to exploit also innovative information sources, as the ones that can be automatically retrieved from photo (e.g., as proposed in Refs. [45,46]).

3.2. Features selection

Once data are available, the second step of the procedure consists in the features selection, which are used to investigate masonry aggregates in the focused area. First, it is worth considering that the proposed method is based on the results obtained from mechanical models (i.e., archetypes), which must be defined on the base of data collected in Section 3.1. Then, these ideal buildings could be arranged according to specific classes, defined under a certain taxonomy (e.g., Refs. [8–10]). On the other hand, META-FORMA-XL does not follow a predefined taxonomy, even because the existing class selection methods are not idealized for masonry aggregates, but for single structural units. In addition, available data could not fit with the requirements of the existing taxonomies. Leaving aside the definition of our archetype (see Section 3.3), the features selection can be processed according to a simple principle, that is, to subdivide the available parameters in *deterministic* and *uncertain*. The deterministic parameters, indicated as P_d, are the certain ones, as well as the ones that cannot be characterized by uncertainty and are reliable. Instead, the uncertain parameters, indicated as P_u, are the ones that cannot be accurately defined and are unreliable. In Table 1, the main useful data for the mechanical modelling purpose are reported and a specific reference to the origin source is added. Obviously, additional parameters can be extracted, especially from CARTIS (e.g., type of mortar), but for purpose of large-scale analysis they can be neglected. As intuitively definable, the items associable to P_d are only the year of construction, the number of storeys and the number of cells composing a masonry aggregate. The other

Table 1
Main available parameters and classification in P_d and P_u. CTR indicates technical regional cartographies.

Data	Source	Type of Parameter (P_u, P_d)
Base Area	CARTIS/CTR	P_u
Floor type	CARTIS	P_d
Year of construction	CENSUS/CARTIS	P_d
Height of the ground floor	CARTIS	P_u
Height of the upper floors	CARTIS	P_u
Number of cells	CTR/CADASTRAL	P_d
Number of storeys	CENSUS/CARTIS	P_d
Percentage of openings at ground floor	CARTIS	P_u
Percentage of openings at upper floors	CARTIS	P_u
Regularity	CARTIS	P_d
Roof type	CARTIS	P_d
Thickness of walls	CARTIS	P_u
Type of masonry	CARTIS	P_u
Sides of structural units	CTR	P_u
Use destination	CARTIS	P_u

items can be classified as P_u, and they characterize the uncertainty sources for the archetypes to be built. Some additional specifications must be provided for P_d parameters. In fact, especially for the number of storeys, within the same aggregate buildings could be disposed in a confused configuration, with some units presenting different heights or even different number of storeys. Nevertheless, it is worth noting that the proposed procedure is aimed at estimating the seismic behaviour of masonry aggregates in historical centres, which are usually built in the same construction period and presenting the same typology, and then the same number of storeys. Obviously, modifications over the time (e.g., superelevation) could lead to observe variations in terms of number of storeys, evidence that is not accounted in this investigation (and in the proposed archetype models) and will characterize further developments. Concerning the number of cells, also for this parameter the structural units could present different geometrical and mechanical features, but it is worth specifying that they are always identifiable considering that clusters in historical centres are usually developed in the same period and with the same construction rules. About P_u, it is worth pointing out that some parameters are more uncertain than others, as for example the Base Area or the Sides of structural units could be defined more precisely than the Thickness of walls or the Percentage of openings at ground and upper floors. At the same time, in the proposed procedure no difference is accounted for among uncertain parameters, which are treated at the same way.

Additional considerations are necessary on the data in Table 1. The parameter Use destination could be intrinsically neglected talking about masonry aggregates, considering that this part of the urban fabric is usually located in historical centres, which present residential scopes. Similar outcome can be provided for the year of construction, which for historical centres dates back to before the beginning of the 20th Century. Therefore, the involved masonry units are usually built only for gravity loads and without any seismic details. Instead, a more refined definition should be provided for the type of masonry. From the CARTIS form, a near-accurate typological definition is obtainable, but for a modelling purpose, it is necessary to provide specific ranges of values that characterize the mechanical properties of the masonry. Thus, in absence of specific material characterization, the type of masonry can be used to retrieve information from the Italian Building Code [47,48], which provides in its Annex the values for masonry typologies defined in CARTIS. In particular, it provides minimum and maximum values for the masonry compressive strength ($f_{c,m}$) and for the masonry tensile strength ($f_{v,m}$). These values can be used also to estimate the masonry young and shear moduli, E_m and G_m respectively, according to the prescriptions provided in Ref. [47]:

$$E_m = 1000 f_{c,m};\ G_m = 0.4 E_m \tag{1}$$

At this point, the above parameters, with the declared exclusions and assumptions, represent the minimum requirements for going to the next step. Nevertheless, if additional data sources are available, they can be introduced in the general framework of the procedure with the aim to refine the input parameters and reduce the uncertainty.

3.3. Archetype definition

Using the data at disposal, the archetype model can be defined. In principle, an archetype is a term coined by Carl Gustav Jung [49] and used in psychology to represents a primitive model, as well as a simplified and unconscious representation of something. By stealing this concept from psychology and transferring it in the field of large-scale seismic analysis, the archetype is a simplified mechanical model that the analyst adopts to succinctly represent the behaviour of a class of buildings, for which some information is uncertain. Obviously, to be faithful to reality, the archetype shall account for all existing geometrical and mechanical uncertainties. In this view, our archetype is a simplified model of a masonry aggregate, which is defined starting from a parametrically defined single building that is replicated according to the desired aggregation form (e.g., row, courtyard).

The proposed archetype model is conceived to account for all uncertainty sources in terms of geometrical and mechanical parameters. For the case at hand, the uncertainties are represented by m types of P_u, where for the ith parameter, n values (v_j) can be defined (variable for each $P_{u,i}$):

$$P_{u,i} = \left[v_1, v_2, \dots, v_j, \dots, v_n\right];\ i = 1, \dots, m; j = 1, \dots, n \tag{2}$$

To this scope, two approaches can be employed: (a) to use a discrete subdivision of the range of values associated to each $P_{u,i}$, which implies the use of a uniform distribution of v_j with the same probability of occurrence; (b) to use a probabilistic distribution of the range of values associated to each $P_{u,i}$, which implies a different occurrence of the of v_j (as for example proposed in Ref. [12]). Taking as reference the P_u in Table 1, the high number of parameters to account for leads to assume the first approach, with a twofold aim: (a) to employ only the available sources of information, e.g., CARTIS form, free databases, Italian Building Code; (b) to reduce the computational effort generated by the combination of each $P_{u,i}$, assuming a specific v_j. In addition, without experimental evidence and with the poor knowledge related to the data at our disposal, to assume different probabilistic distributions from the uniform one could attribute higher weight to specific v_j than the reality, biasing the subsequent overall evaluations. Then, to make the proposed archetype, each $P_{u,i}$ with a v_j must be combined with the r types of $P_{d,z}$, where for the zth parameter, s values (v_u) can be defined (variable for each $P_{d,z}$):

$$P_{d,z} = \left[v_1, v_2, \dots, v_u, \dots, v_s\right];\ z = 1, \dots, r; u = 1, \dots, s \tag{3}$$

Thus, an archetype model (indicated as $\mathbb{V}$) can be mathematically defined as a combination of $P_{d,z}$ and $P_{u,i}$ with the related values, and expressed as the union of values belonging to different vectors:

$$\mathbb{V} = \bigcup_{z=1}^{r} \bigcup_{i=1}^{m} P_{d,z}\left(v_u\right) P_{u,i}\left(v_j\right) \tag{4}$$

The discussion provided for the single unit can be extended to the masonry aggregate, where Equations (2)–(4) are valid. For the variation of the couple parameter-value and of the masonry aggregate modelling (i.e., replication of structural units according to a predefined form), it is possible to exploit the same principles provided in the original version of META-FORMA [4], in which a fully automated procedure was provided based on the relation between POR2000 [17] and Matlab [16]. Avoiding to report details about coding aspects, it is worth pointing out that the idea herein proposed aims to replicate the same structural unit more times according to the selected $P_{d,z}$ and the type of aggregation. This means that the values of each $P_{u,i}$ is assumed as same for all structural units composing the masonry aggregate. This is a strong assumption, considering that, for example, it is not possible to variate the height of the storeys within the same aggregate, situation that can occur in real-life cases. On the other hand, with the proposed methodology it is possible to variate the geometry of the structural units, by modifying both base area and aspect ratios between the sides or the disposition of the internal units. To the above simplification corresponds the possibility to systematically account for the variability of each parameter, by exploiting the computational performance of an automated tool that generates a high number of models at the low time costs. As a matter of fact, through the adopted approach, it is possible to generate a total number of models, N_m, equal to:

$$N_m = \prod_{z=1}^{r} \prod_{i=1}^{m} \Psi\left(P_{d,z}\right) \Psi\left(P_{u,i}\right) \tag{5}$$

where Ψ is the function indicating the cardinality of the vectors identified by each $P_{d,z}$ and $P_{u,i}$. The greater the number of values that each parameter assumes, the greater N_m will be. Once models are available, global and local analyses can be carried out, as reported in Sections 3.4 and 3.5, respectively.

3.4. Global analysis

Concerning the global analysis, the seismic behaviour of archetype models is investigated accounting for the in-plane behaviour of the masonry walls. Regarding the modelling of the single structural unit, the software used is POR2000 [17], based on the POR method [50] and that employs the recent evolutions of the code in Refs. [51,52]. In detail, the method adopts an equivalent frame approach in which the only resistant elements are represented by the masonry piers and the contribute of the masonry spandrels is neglected. The zones where the failure modes occur are localized in the piers that are connected to the spandrels through rigid nodes. Following the concepts in the original method, a box-like behaviour is accounted in the archetype model, which implies two main assumptions: (a) shear-type behaviour, with constrained rotations at the top and at the bottom of the masonry piers; (b) the floors are subjected only to in-plan rigid roto-translations. The above hypotheses are reliable if good connections exist among masonry piers, which implies a good torsional behaviour of the building. This could represent a limit for the use of the method, especially for those buildings without presenting good connections among masonry panels. Nevertheless, for purpose of aggregates, the absence of wall connections could be overcome by the group effect given by the clustering of structural units (especially in the central units). In addition, it is worth reminding that the proposed modelling is aimed at simulating archetypes, which can be models with a certain simplification degree. The assumptions at the base of the models provide a high efficiency in the analysis resolution, which makes the software very fast, as an important skill in large-scale analysis. Another aspect to highlight about the selected modelling method is the consideration of the openings, which are taken into account with some modifications, by employing a reduction of the effective height of the masonry piers by means of a specific diffusion angle of stress in the near of openings and by introducing a stiffness modification in the spandrel located above and under the openings. Regarding the nonlinear behaviour of the structural elements, each masonry pier is modelled through a specific behaviour, for which a bilinear perfectly elasto-plastic constitutive law is usually assigned, defined in terms of strength and ductility. The elastic behaviour is defined according to the stiffness of the masonry panel and

its maximum is identified as the displacement (yielding displacement, d_y) at the ultimate shear, V_u, or bending moment, M_u values. The value of the V_u is related to the axial stress, which the software automatically attributes to each masonry panel according to the acting loads and to the stiffness, which is ruled by the theory of the Timoshenko beam. After the yielding, the displacement constantly increases up to the failure that can occur for ductile, $d_{NC,D}$ or brittle, $d_{NC,S}$ failures, where NC indicates the near-collapse limit-state. After achieving $d_{NC,D}$ or $d_{NC,S}$, the masonry panel can be considered as collapsed. With this regard, when pushover analysis is employed, the software solver evaluates for each step of analysis the values of V_u and M_u and a check of the panel is performed in terms of displacement. When the displacement of the panels increases (and then collapses occurs), the structure progressively loses its bearing capacity, and the analysis ends when the base shear achieves the minimum residual capacity. While evaluation the base shear as the sum of all the panels base shear, the correspondent displacement is defined through an energetic equivalence criterion based on deformation work, making the results independent from the choice of a control point. For the above reported information, the software does not consider a cracked section, but follows a different decay model, given by the plasticity model assigned to the panel.

Once defined the modelling assumptions, the employed structural software allows to perform nonlinear static analyses along multiple directions by defining an angle of incidence of the seismic action measured with respect to the global reference system (i.e., from 0° to 360°, with an incremental step of 45°). For the case at hand, of interest are the two main directions (defined as X and Y) and both verses, corresponding to 0° and 180° for X direction and 90° and 270° for Y direction. For each analysis, according to the prescriptions provided by the Italian Building Code [47], nonlinear static analyses are performed through two load profiles, that is, the uniform (proportional to the mass of the storeys) and the inverse triangular (proportional to the height of the storeys) ones. As results of the analyses, the relationship between the global capacity and the demand of each archetype (C/D_G ratios, where G stands for global) is provided, for each desired limit-state. Through the tool developed in Ref. [4], the analyses can be run in serial, by obtaining the values of C/D_G ratios for each direction, each load profile, and each limit-state. Retaining the subdivision per direction and limit-state, the selected C/D_G ratios to be processed in the fragility analysis (see Section 3.6) are the lower ones between the two versus and between the two load profiles. In summary, from each archetype model, the global analysis provides eight values of C/D_G ratios (4 limit-states and 2 main directions).

To quantify the C/D_G ratios, the software compares capacity and demand spectra following the method reported in Ref. [47], and for which values of demand and capacity expressed in terms of PGA are provided. To identify the achievement of the limit-states, the software opts to assume horizontal displacements computed as fraction of the pier height, h_p. According to Ref. [47], the immediate occupancy (IO) limit-state displacement, $d_{IO\text{-}G}$, is defined as

$$d_{IO-G} = 0.002h_p \tag{6}$$

while the NC limit-states, $d_{NC,D}$ and $d_{NC,S}$, are defined as

$$d_{NC,S-G} = 0.005h_p \tag{7}$$

$$d_{NC,D-G} = 0.010h_p \tag{8}$$

On the base of the values defined in Equations (6)–(8), the limit-states are following defined.

- Operativity limit-state (O): exceeded when the first pier achieves a displacement equal to 66% of $d_{IO\text{-}G}$.
- Immediate occupancy limit-state (IO): exceeded when the first pier achieves a displacement equal to $d_{IO\text{-}G}$.
- Life-safety limit-state (LS): exceeded when the first pier achieves a displacement equal to 75% of $d_{NC,D\text{-}G}$.
- Near-collapse limit-state (NC): exceeded when the first pier achieves a displacement equal to $d_{NC,D\text{-}G}$ or $d_{NC,S\text{-}G}$, or when the residual capacity of the structural system is equal to the 80% of maximum base shear.

By using the approach above described, C/D_G ratios are available for the entire sample of archetype buildings, assuming as value of the seismic demand a representative one of the area under investigation.

3.5. Local analysis

Concerning local analyses, the seismic behaviour of archetype models is investigated in order to take into account the occurrence of damages related to out-of-plane mechanisms in masonry walls. For purpose of automatization, the local analysis module extracts from the input files generated through the global analysis modules (for more information see Ref. [4]) the useful features to perform a specific investigation on the out-of-plane behaviour of masonry panels.

To this scope, a macro-block model is considered which is based on the hypothesis that, when the mechanism activates, the structure separates into rigid blocks thanks to the development of macro cracks along which all the deformation is concentrated. Each block is assumed to be infinitely rigid and resistant. This approach is frequently adopted for modelling out-of-plane collapse, as reported in Ref. [53] and it is based on the assumption of a bad connection between orthogonal walls, which implies the occurrence of simple rocking and vertical flexure mechanisms, as shown in Fig. 2. Therefore, the contribution of perpendicular walls is neglected. This conservative assumption is made since the information on the quality of the connection among walls is not easily obtained for large-scale vulnerability analyses. For the case at hand, each archetype can be subjected to both mechanism types involving one or more storeys. While for the simple rocking case the positions of the macro crack are assigned at the bottom of each storey, for the vertical flexure the macro crack is positioned in order to device the worst case.

For each mechanism, the nonlinear kinematic approach is adopted to obtain a capacity curve in terms of the applied seismic force and the displacement of a reference point. To this end, the schemes shown in Fig. 3 are considered. In particular, all the weights in-

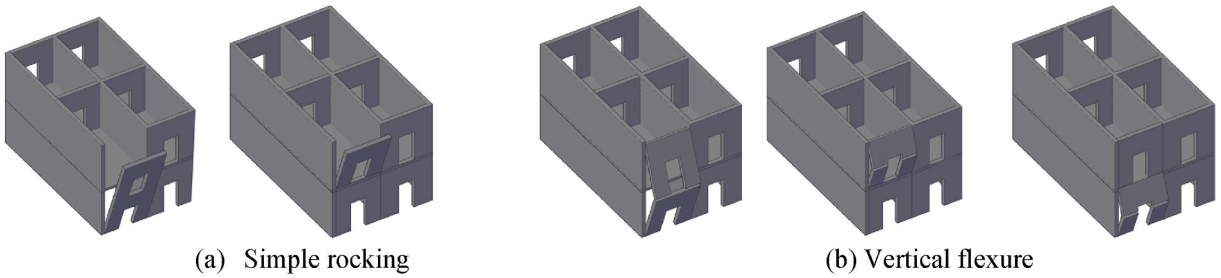

Fig. 2. Local mechanisms considered in the analysis: (a) simple rocking; (b) vertical flexure.

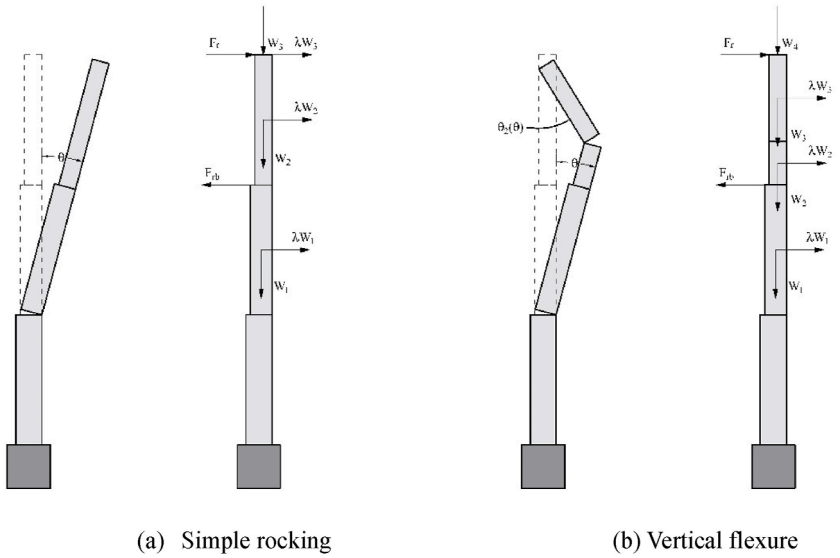

Fig. 3. Local mechanism schemes: (a) simple rocking; (b) vertical flexure.

volved are considered as vertical forces, W_i, applied at generical points indicated as $X_{w,i}$. The seismic action is assumed as proportional to the weights by means of a multiplier, λ, and still applied at points $X_{w,i}$. The schemes in Fig. 3 report also the presence of the horizontal forces due to tie-rods, F_{tr}, ring beams, F_{rb}, and thrusting roof, F_r. The involved weights are comprehensive of masonry self-weight and slab reactions.

On this basis, the work of the applied forces can be estimated as

$$W(\lambda, \vartheta) = \sum_i F_i(\lambda)\, d_i(\vartheta) \tag{9}$$

where $F_i(\lambda)$ collects the vertical and horizontal components of the ith force, while $d_i(\vartheta)$ represents the displacement vector of the point where $F_i(\lambda)$ is applied. The contribution of perpendicular walls can be easily considered by adding the resistance to the summation in Equation (9). The displacement $d_i(\vartheta)$ nonlinearly depends on the unique kinematic parameter, the rotation ϑ, which defines the assumed local mechanism. Such a dependence can be expressed through a Taylor expansion up to the desired order. In the present case, it is sufficient to use a second order expansion.

The equilibrium equation, and then the capacity curve relating ϑ and λ, can be obtained by imposing the stationarity condition for $W(\lambda,\vartheta)$, as shown in Equation (9). The obtained capacity curve is then transformed in that of an equivalent single-degree-of-freedom model, by using the capacity spectrum method approach [54,55]. The kinematical parameter ϑ is linked to the parameter ϑ^* of the equivalent system through the relation [47,48].

$$\vartheta = \Gamma\vartheta^* = \vartheta^* \frac{\sum_i \boldsymbol{F}_i \boldsymbol{d}_i(\vartheta = 0)}{\sum_i \boldsymbol{F}_i \boldsymbol{d}_i(\vartheta = 0)^2} \tag{10}$$

while the acceleration of the capacity curve is obtained as

$$a\left(\vartheta^*\right) = \frac{g\lambda\left(\vartheta^*\right)}{e^*}, \tag{11}$$

where e^* is the mass participation rate for the local mechanism evaluated as

$$e^* = \frac{\left(\sum_i \boldsymbol{F}_i \boldsymbol{d}_i\left(\vartheta = 0\right)\right)^2}{\sum_j W_j \sum_i \boldsymbol{F}_i \boldsymbol{d}_i (\vartheta = 0)^2} \tag{12}$$

The limit-states, representing the damage levels due to local mechanisms, are defined in terms of fraction of the maximum displacement, indicated as out-of-plane d_0, namely the value of the displacement corresponding to a zero value of λ. To define limit-states thresholds, and neglecting the achievement of the O limit-state (this is an elastic state, and the mechanisms does not occur), IO, LS and NC, identified with $d_{IO\text{-}L}$, $d_{LS\text{-}L}$, $d_{NC\text{-}L}$, respectively, are reached according to the following Equations:

$$d_{IO-L} = 0.1 d_0 \tag{13}$$

$$d_{LS-L} = 0.4 d_0 \tag{14}$$

$$d_{NC-L} = 0.6 d_0 \tag{15}$$

The performance point in terms of displacement demand d_{Dk} for the kth limit-state due to local mechanisms, related to the spectral displacement d_k and acceleration a_k on the equivalent system, is evaluated as

$$d_{Dk} = \left(\frac{T_{sk}}{2\pi}\right)^2 S_d\left(T_{sk}\right), \tag{16}$$

where $S_d(T_{sk})$ is the pseudo-acceleration response spectrum evaluated for the period T_{sk}, obtained, for each limit-state, as

$$T_{sk} = \alpha\, \pi \sqrt{d_k a_k} \tag{17}$$

being α a coefficient depending on the limit state, as shown in Refs. [47,48].

Finally, for a given direction of the seismic action and for each limit-state, it is possible to obtain the ratio d_k/d_{Dk}. The minimum among all these ratios evaluated for all the building facades and local mechanisms provides the C/D_L ratio. As a final consideration, it is worth mentioning that the local nature of this analysis implies that the results do not depend on the number of cells of the aggregate. In addition, as further assessment of the proposed local analysis, all evaluations are made by considering the possible presence or absence of the ring beam.

3.6. Seismic fragility analysis and comparison between global and local mechanisms

The obtained results in Sections 3.4 and 3.5 can be processed to derive global and local fragility curves. In general, fragility curves express the probability that the structure (or a part of it) exhibits to exceed a specific deformation condition, i.e., limit-state. It is worth noting that the proposed approach for both global and local analysis is simplified and, in some cases, could reproduce the real conditions of real buildings in historical centres (e.g., presence of flexible slabs, influence of floor beam effects). On the other hand, the proposed approach employs archetypes buildings, which are simplified models with a certain degree of simplification (as for example, global analysis is performed by using a single rigid floor at each level and monitoring a single control point). Although simplified, the POR method fits well with the purpose of the paper, which aims to predict seismic fragility of masonry aggregates in a simple and fast way and to develop risk priorization strategies. In addition, a full investigation of the uncertainties can be performed, employing a reasonable time of analysis and computational effort. From the mathematical point of view, a fragility curve is described by a cumulative distribution function (CDF) reporting the relation between a selected seismic intensity (defined through an IM) and the related probability of failure, P_f. Hence, the fragility function can be expressed as

$$P\left(failure|IM = x\right) = \Phi\left(\frac{\ln\left(\frac{x}{\mu}\right)}{\beta}\right) \tag{18}$$

where $\Phi(\bullet)$ is the standard normal CDF, x is a value of IM and assume increasing values, μ and β are the median and the dispersion of the CDF, respectively, the failure identifies the condition beyond which the limit-state is exceeded.

For the case at hand, the failure, which is usually related to a capacity parameter, is not represented by a specific EDP, but the output of the analysis is the structural response, identified as C/D_G and C/D_L ratios, for global and local analysis, respectively. For each analysis, it is possible to observe if the values of C/D_G and C/D_L ratios are greater or lower than 1, which means "not collapsed" or "collapsed", respectively. Hence, to build the fragility curves, it is worth employing the concept of multi stripe analysis [56], which allows to investigate the structural response at increasing values of IMs, denoting if the collapse occurs or not. Under this method, the

values of C/D_G and C/D_L ratios, evaluated for the site seismicity of the focused area, must be recomputed by increasing the seismic demand. Hence, the operations described in Sections 3.4 and 3.5 must be repeated more times, for discrete increments of the IM, in order to achieve the collapse.

At this point, the fragility function could be evaluated on the N_m of archetypes, but a smart subdivision can be employed, in order to observe the variability of fragility curves for the proposed archetypes. As a matter of fact, the models can be subdivided in subsamples, with a number of models indicated as $N_{m,s}$, where fixed values v_u of $P_{d,z}$ are selected and all values v_j of $P_{u,i}$ are varied. In this way, all the uncertainty sources are considered, while differences among different evident structural conditions can be appreciated (e.g., difference between row masonry aggregates having 2 and 3 structural units). For each direction and each limit-state, $N_{m,s}$ is equal to

$$N_{m,s} = \sum_{z=1}^{r} P_{d,z}\left(v_u\right) \prod_{i=1}^{m} \Psi\left(P_{u,i}\right) \tag{19}$$

On the results obtained by the subsamples of models, the observation of the C/D_G and C/D_L ratios brings to define the probability of having collapse ($N_{m,s\text{-}c}$) out of the $N_{m,s}$, for a given IM. Assuming the independence among the obtained results, this latter probability can be defined through the maximum likelihood approach [57]. For different values of IM, fragility curves can be estimated by maximizing the likelihood of the subsamples, which in turn is obtained as the product of binomial probabilities (with parameters $N_{m,s\text{-}c}$ and $N_{m,s}$) for each IM value. In other words, following the Baker proposal, the fragility function parameters are determined as

$$\left\{\hat{\mu},\hat{\beta}\right\} = \arg\max_{\mu,\beta} \sum_{w=1}^{l} \left\{ \ln\left(\begin{array}{c} N_{m,s \mid IM=x_w} \\ N_{m,s-c \mid IM=x_w} \end{array} \right) + N_{m,s-c \mid IM=x_w} \ln \Phi\left(\frac{\ln\left(\frac{x_w}{\mu}\right)}{\beta} \right) + \right.$$

$$\left. \left(N_{m,s \mid IM=x_w} - N_{m,s-c \mid IM=x_w}\right) \ln\left(1 - \Phi\left(\frac{\ln\left(\frac{x_w}{\mu}\right)}{\beta}\right)\right) \right\} \tag{20}$$

where w and l are indexes indicating the specific value and the total number of explored IMs, respectively. Obviously, Equation (15) can be applied for both global and local mechanisms, to compute the P_f of the subsample of models and then of the typological masonry aggregate, which represents the output of META-FORMA-XL. Naming the P_f for global mechanisms as $P_{f,G}$ and the P_f for local mechanisms as $P_{f,L}$, for each direction and limit-state, the overall P_f, to be evaluated for each value of IM, is defined as

$$P_f = \max\left(P_{f,G}, P_{f,L}\right) \rightarrow \forall \text{direction, limit} - \text{state} \tag{21}$$

4. Case study

The proposed procedure was applied to the row masonry aggregates in the historical centre of Foggia, Puglia, Southern Italy. In the next Sections, a description of the reference context is provided, together with the application of the proposed procedure and the validation of the methodology with a real-life case study.

4.1. Description of the reference urban context

The municipality of Foggia is located in the northern part of the Puglia region, Southern Italy and it presents a medium seismicity with a value of PGA ranging from 0.13 to 0.15g for a probability of exceedance of 10% in 50 years. The existing building stock is composed by about 7000 buildings, equally subdivided in RC and masonry structural units [58]. More than the 75% of the entire building stock was built before the first seismic classification, that is, the 1980.

Starting with the application of the proposed procedure, a data collection was performed. In particular, the CARTIS form was compiled to identify the homogeneous TCs. The results of the above interview-based approach suggest that about 12 TCs are available, in which the 50% of TCs contained the 95% of the entire building stock. Thus, looking at the residential buildings, 6 TCs can be focused (the remaining 6 TCs are located in the rural zone around the built area), as displayed in Fig. 4. The TCs named C01 and C02 (red and blue areas in Fig. 4) constitute the historical centre of the municipality, where more than the 50% of the total number of masonry buildings is present. As occurs in most of the Apulian historical centres, the buildings are organized in aggregate configuration and disposed as a central shape nucleus [59]. The TC named C03 (green area in Fig. 4) is the first expansion zone, and it is also constituted by masonry buildings disposed in aggregate. The TCs named C04, C05, and C06 (orange, violet and yellow areas in Fig. 4, respectively) are the recent expansion zones and they are predominantly constituted by RC buildings.

Of interest for the scope of this paper is the part of the historical centre, which is identified in the TCs named C01 and C02. Nevertheless, also C03 could be considered, but it is worth noting that the disposition of masonry buildings is different from the previous TCs. As a matter of fact, C01 and C02 present buildings disposed in row, while C03 present buildings predominantly disposed in courtyard. On this base, for the scope of our investigation, only C01 and C02 were focused, and about these areas other data sources were retrieved. As suggested in Section 3.1, some freely databases were exploited and then, the census and CTR data were examined for the TCs under investigation. Fig. 5 shows the data collected and subdivided in GIS layers, reporting then census, CTR and CARTIS representation for C01 and C02.

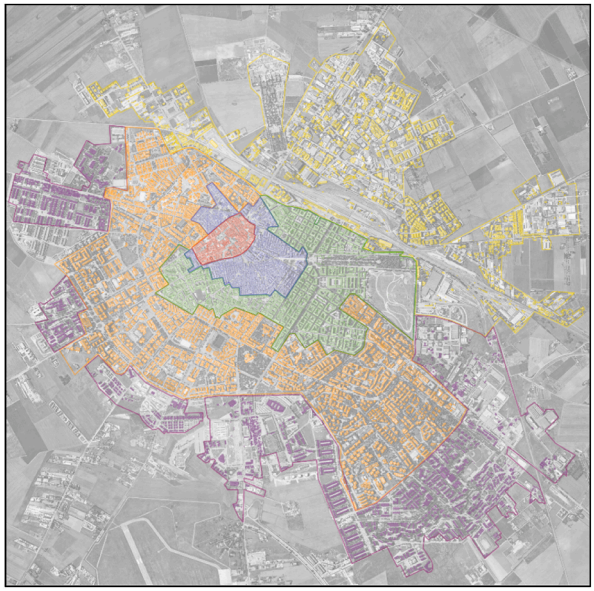

Fig. 4. Definition of the TCs for the municipality of Foggia, Southern Italy. The historical centre is outlined through the red and blue areas, which are C01 and C02, respectively. Green, orange, violet and yellow areas represent C03, C04, C05, and C06, respectively. (For interpretation of the references to colour in this figure legend, the reader is referred to the Web version of this article.)

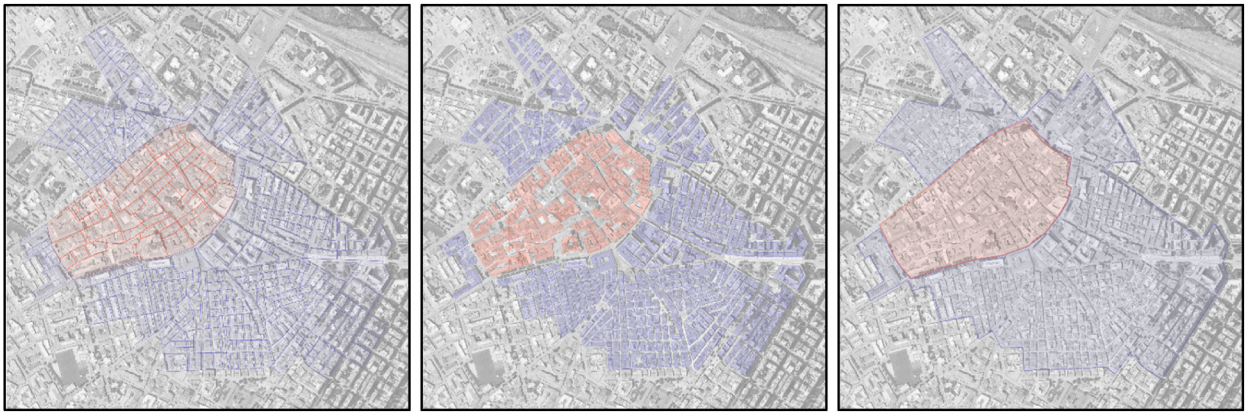

Fig. 5. Data collected about the historical centre of for the municipality of Foggia. From left to right, for the TCs named C01 and C02 (red and blue areas, respectively), are reported data about Census, CTR, and CARTIS. (For interpretation of the references to colour in this figure legend, the reader is referred to the Web version of this article.)

Comparing C01 and C02, the main difference resides in the year of construction and in the type of aggregation. C01 dates back to the medieval period, while C02 dates back to the 18th century. In addition, C01 presents a disordered urban fabric, while C02 is characterized by a regular distribution of the buildings stock with row masonry aggregates containing a different number of structural units. To apply META-FORMA-XL, the regular part of the historical centre was considered, and then the focus was shifted to C02.

4.2. Application of the proposed procedure to row masonry aggregates in c02

From the compilation of the CARTIS form and the integration of the other data sources for C02, a clear identification of typological features was obtained, according to the parameters reported in Table 1. Excluding some parts of the existing building stock, regular row masonry aggregates were observed, with a number of structural units varying from 2 to 4 cells, with some sporadic cases presenting 5 and 6 cells. Fig. 6 shows the zooms on specific masonry aggregates of the historical centre, reporting the variation of the number of cells within the rows.

As typological description, the masonry aggregates present in plan and in heigh regularity, a number of storeys ranging from 1 to 2, shorter sides ranging from 10 to 15 m with an area ranging from 70 to 100 m^2, a structural masonry constituted by square stone blocks and a little difference between the height of the first and the upper floors (where the storeys are 2). A detailed summary of the range values for the parameters reported in Table 1 and obtained from the above performed data fusion is reported in Table 2.

Fig. 6. Identification of the number of cells within the row masonry aggregates in C02 of the municipality of Foggia.

Table 2
Ranges of values for the parameters in Table 1 and defined according to the data fusion among census, CTR and CARTIS data.

Parameter	Range values
Base Area	70–100 (m^2)
Floor type	Rigid slab
Year of construction	1861–1919
Height of the ground floor	3.50–4.00 (m)
Height of the upper floors	3.00–3.50 (m)
Number of cells	2–6
Number of storeys	1–2
Percentage of openings at ground floor	20–30 (%)
Percentage of openings at upper floors	10–20 (%)
Regularity	In-plan and in eight
Roof type	Flat roof
Thickness of walls	0.25–0.50 (m)
Type of masonry	Square stone block
Sides of structural units	10–15 (m)
Use destination	Residential

At this point, the feature selection described in Section 3.2 can be processed, by subdividing the parameters in P_d and P_u with the related values. Following the indications in Section 3.2, the parameters floor type, year of construction, number of cells, number of storeys, regularity, roof type, and use destination are the $P_{d,z}$, while the other are $P_{u,i}$. For purpose of archetype modelling, only the number of cells and the number of storeys are considered as variables and then presenting different v_u, while the other parameters are assumed as fixed for all archetypes. Regarding the $P_{u,i}$, a refined subdivision of the range values in Table 2 was selected, in order to employ a uniform distribution of v_j with the same probability of occurrence.

Some specifications are required for each parameter in play. First, as shown in Fig. 6, the number of cells should range from 2 to 6, but for sake of completeness, we investigated also the single structural unit. This could suggest some insights at the end of META-FORMA-XL application. Regarding the height of ground and upper floors, a high discretization was employed, considering that are fundamental parameters for the evaluation of local mechanisms. Same approach was used for the discretization of the percentage of

openings of ground and upper floors, as important parameter for the evaluation of global mechanisms. Thickness of the walls was discretized considering a little step of 5 cm, considering its importance in both local and global mechanisms evaluation. For the type of masonry (important in the global mechanisms estimation), the prescriptions provided in Ref. [47] were assumed (with the related quantities about the moduli E_m and G_m) and, looking at the identified type of masonry, the range of values corresponding to regular limestone masonry was employed with a light discretization, both for $f_{c,m}$ and $f_{v,m}$. In the end, also the global geometrical parameters base area and side of the structural units were assumed with a light discretization, considering that the combination of the values of these parameters can overall cover the configurations of the investigated structural cells. Table 3 reports v_u and v_j for $P_{d,z}$ and $P_{u,i}$, respectively, to employ at the base of the archetype modelling generation.

An additional parameter must be still mentioned for the evaluation of local mechanisms, that is, the ring beam, as reported in Section 3.4. This parameter is a $P_{d,z}$ assuming only two possible v_u: present or absent. Although ring beam was not mentioned in Table 3 (also because it is not evincible from the available sources), it was systematically considered in the local analysis, in order to assess the output of META-FORMA-XL in presence or absence of this important structural detail. Obviously, according to our modelling assumptions, the ring beam does not influence the global behaviour.

Given the input parameters and the discretization values, the phase of archetype modelling can be performed. Using the rules defined in META-FORMA [4] for the modelling, and the combination of the parameters defined in Equation (5), the N_m is equal to 629856. In this count, the values of $f_{c,m}$ and $f_{v,m}$ are not both considered in the combination, because the definition of the masonry type is defined by both parameters (e.g., a masonry having $f_{c,m}$ equal to 2.041 MPa was supposed to have a $f_{v,m}$ equal to 0.102 MPa). As an example of the criteria for the archetype modelling generation, Fig. 7 shows a couple of cases to observe the geometrical variation obtained by assuming $P_{d,1}$, the number of storeys, and as $P_{d,2}$, the number of cells, equal to 1 and 3, respectively for the first case, and equal to 2 and 6, respectively for the second case. As can be seen, a consistent variation of the global geometry was obtained for both cases, considering for example that the span length was fixed with a maximum of 6 m (especially to avoid unreal situations) and

Table 3
Definition of v_u and v_j for $P_{d,z}$ and $P_{u,i}$, respectively, to employ in the archetype modelling campaign. $P_{d,z}$ and v_u values are reported in bold and italic style.

Parameters ($P_{d,z}$, $P_{u,i}$.)	Values (v_u, v_j)
Base Area (m^2)	70–85 – 100
Height of the ground floor (m)	3.50–3.60 – 3.70–3.80 – 3.90–4.00
Height of the upper floors (m)	3.00–3.10 – 3.20–3.30 – 3.40–3.50
Number of cells (–)	***1 – 2 – 3 – 4 – 5 – 6***
Number of storeys (–)	***1–2***
Percentage of openings at ground floor (%)	20–25 – 30
Percentage of openings at upper floors (%)	10–15 – 20
Thickness of walls (m)	0.25–0.30 – 0.35–0.40 – 0.45–0.50
Type of masonry - $f_{c,m}$ (MPa)	2.041–2.653 – 3.265
Type of masonry - $f_{v,m}$ (MPa)	0.102–0.148 – 0.194
Sides of structural units (m)	10–12 – 15

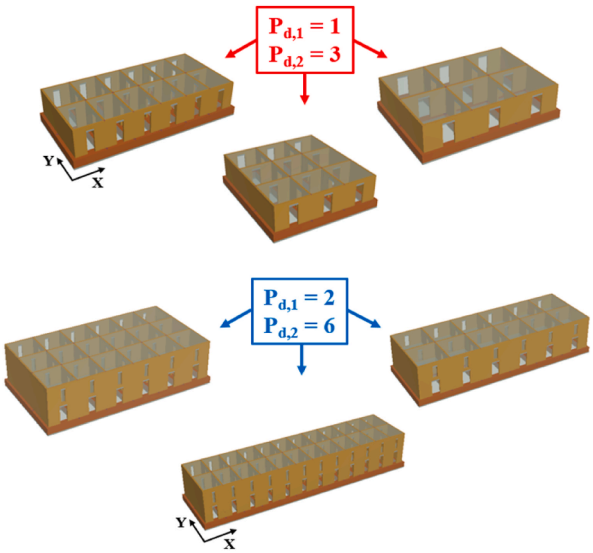

Fig. 7. Examples of variation of the geometrical features of archetypes using META-FORMA [4], and obtained assuming as $P_{d,1}$ the number of storeys and as $P_{d,2}$ the number of cells with v_u equal to 1 and 3, respectively (red square), and assuming, as $P_{d,1}$ the number of storeys and as $P_{d,2}$ the number of cells with v_u equal to 2 and 6, respectively (blue square). An indication about the global reference system is added, identifying X and Y directions. (For interpretation of the references to colour in this figure legend, the reader is referred to the Web version of this article.)

the number of internal bays and their length in both main directions were determined according to the values of the base area and the length of the structural side.

Once generated archetype models, local and global analyses can be carried out, according to the descriptions in Section 3.4 and 3.5. Downstream of this stage, fragility analysis accounting for both global and local mechanisms can be performed. To this scope, the subdivision of N_m archetypes in subsample, $N_{m,s}$ was performed, by grouping all models according to a fixed value of number of storeys and number of cells. Thus, the value of $N_{m,s}$ is equal to 52488. Global and local analyses were carried out on each subsample, and fragility curves were derived by applying the Baker methodology (i.e., counting the $N_{m,s\text{-}c}$ over the $N_{m,s}$ for increasing levels of IMs, identified like PGA, and maximizing the likelihood through the formulation in Equation (20)).

The results were obtained for each limit-state, each direction, and each failure mechanism (fragility for local mechanisms were evaluated with and without ring beams). The output of META-FORMA-XL is reported in Figs. 8 and 9, subdividing results in X and Y directions, respectively. Figs. 8 and 9 report in each row 4 graphs, one for each limit-state, and in each column 6 graphs, one for a specific number of cells. In each graph, 6 curves are reported, representing the fragility curve accounting global mechanisms and the fragility curves accounting local mechanisms with and without ring beam, for 1 and 2 storeys. Only for the O limit-state, there are 3 curves, given the impossibility to compute local mechanisms for this condition, according to the adopted methodology.

Looking in detail the obtained curves, several outcomes can be highlighted. It is worth noting that, for the same masonry panel, local and global collapses do not occur in the same direction, which implies that the results in Fig. 8 report fragility curves for in-plane collapses in X direction of the panels oriented in X direction and out-of-plane collapses in X direction of the panels oriented in Y direction (same observation is valid for Y direction). First, as expected, both for local and global mechanisms fragility curves present increasing values of μ going from the O limit-state to NC one. Comparing global and local fragility curves and assuming a value of IM, in X direction the local curves present a higher $P_{f,L}$ than $P_{f,G}$ when the ring beam is not considered, while the reverse occurrence is observed when the ring beam is accounted for. Instead, in Y direction, $P_{f,L}$ considering or not the ring beam is always higher than $P_{f,G}$. Observing global fragility curves of models made by 1 cell, it is worth observing that in our archetypes, the openings are placed in the masonry panels oriented in X direction, which provokes a higher $P_{f,G}$ than the one obtained in Y direction. Hence, by varying the number of cells, an evident trend can be observed in global mechanisms. As a matter of fact, in X direction the $P_{f,G}$ decreases as the number of cells increases, while in Y direction the $P_{f,G}$ increases as the number of cells increases. Note that the increment of fragility in Y direction is faster than the decrement of fragility in Y direction. Concerning local fragility curves, according to the method described in Section 3.5, the variation of the number of cells in archetypes does not influence results, considering that the analysis was performed panel-by-panel. In the end, within each graph, as the number of storeys varies, the fragility for global mechanisms changes, having a higher $P_{f,G}$ for archetypes with 2 levels. Instead, for local mechanisms, the differences are not that obvious, having that, without considering ring beam the fragility is almost same for both main directions, while when considering ring beam, the fragility presents a higher $P_{f,L}$ for archetypes with 1 storey in X direction and an almost same result in Y direction.

4.3. Numerical validation

With the aim to validate the obtained output from META-FORMA-XL, a real-life case study of masonry aggregate was investigated. In detail, the surveyed structures are located always in the historical centre of Foggia, and the focused masonry aggregate is composed by 5 buildings (cells) disposed in row. All buildings present 1 storey with the same height, but the in-plan dimensions vary. The photo of the entire aggregate is reported in Fig. 10, while in Fig. 11 the drawings of the elevation view and of the planimetric distribution of panels are depicted. The detailed geometrical survey allows to categorize this case study under the ranges above identified to generate the analysed archetypes. It is worth noting that, at disposal of the authors, most of the geometrical features are available, while only the mechanical properties are unknown (i.e., $f_{c,m}$ and $f_{v,m}$). On the other hand, some geometrical features here accounted could be affected by uncertainty, such as the thickness of the walls. For this latter parameter, the external walls were considered to vary from 40 to 50 cm, while the internal walls were considered to vary from 25 to 30 cm. Hence, the fragility analysis of the real row masonry aggregate can be processed, accounting in the numerical model for the variation of the mechanical properties (the same values in Table 3 can be exploited, given that the observed masonry type is the same of the typological investigation) and of the wall thickness. Analogously to the established criteria to investigate typological aggregates, the study of the real cases study was carried out by considering each limit-state, each main direction, and global and local mechanisms. No visual information was detected for the presence or absence of the ring beam, and for this reason, the analysis was performed with and without this structural detail.

Thus, if the output of META-FORMA-XL is reliable, the local and global fragility curves shown in Figs. 8 and 9 should represent the seismic behaviour of the real masonry aggregate. On the other hand, it is almost impossible to derive the same result from the typological and the detailed analysis, that is, it is impossible that a specific fragility curve taken from Fig. 8 or 9 perfectly matches the same output for the real masonry aggregate. To overcome this limit, a spindle of typological fragility curves can be derived, which represents, on one hand, the minimum and the maximum limits for each typological fragility curve and, on the other hand, should enclose the output provided by the detailed analysis on the real case study. In Table 4, the parameters employed to derive typological minimum and maximum fragility curves (and then, the desired spindle) are reported, where the varied parameters are selected among the uncertain ones (i.e., $P_{u,i}$). To define the minimum fragility curves, the assumed parameters are the minimum values for thickness of walls and for mechanical parameters of masonry, and the maximum values for the percentage of openings at ground and upper floors. Instead, to define the maximum fragility curves, the assumed parameters are the maximum values for thickness of walls and for mechanical parameters of masonry, and the minimum values for the percentage of openings at ground and upper floors. The remaining parameters are varied according to the values defined in Table 3. Obviously, the process can be repeated for each combination of $P_{d,z}$ but, for the case at hand, it was performed for a number of storey equal to 1 and for a number of cells equal to 5 (according to the investigated case study), considering each limit-state, each direction, and each failure mechanism.

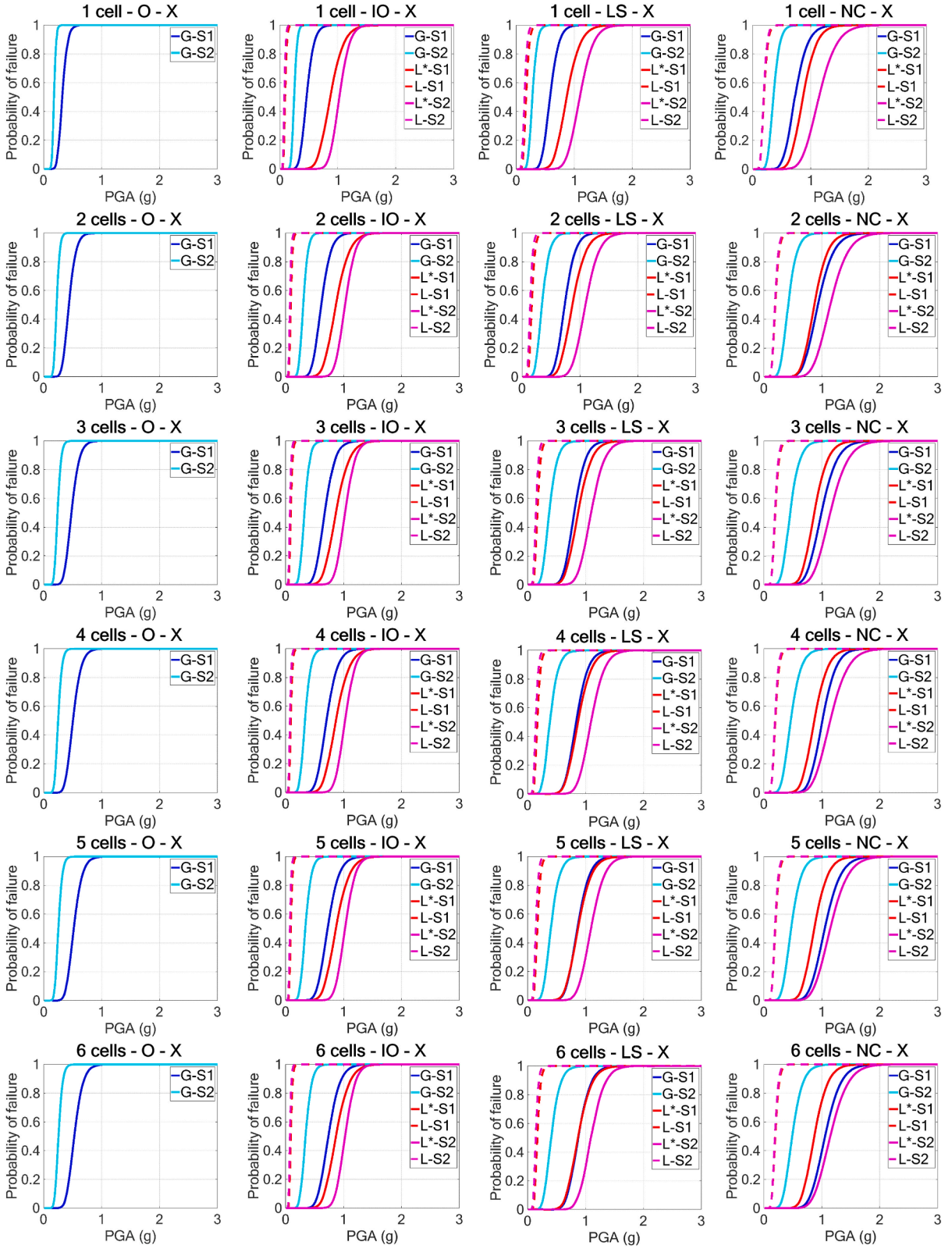
1 cell - O - X
1 cell - IO - X
1 cell - LS - X
1 cell - NC - X
2 cells - O - X
2 cells - IO - X
2 cells - LS - X
2 cells - NC - X
3 cells - O - X
3 cells - IO - X
3 cells - LS - X
3 cells - NC - X
4 cells - O - X
4 cells - IO - X
4 cells - LS - X
4 cells - NC - X
5 cells - O - X
5 cells - IO - X
5 cells - LS - X
5 cells - NC - X
6 cells - O - X
6 cells - IO - X
6 cells - LS - X
6 cells - NC - X
Probability of failure
PGA (g)
G-S1
G-S2
L*-S1
L-S1
L*-S2
L-S2

Fig. 8. Fragility curves in X direction, accounting for local and global mechanisms (with and without ring beam), reported for each limit-state and varying the number of storeys and number of cells. G stands for global, L stands for local without ring beam, L* stands for local with ring beam. 1S and 2S indicate 1 storey and 2 storeys, respectively.

At this point, the procedure in META-FORMA-XL can be repeated, evaluating fragility curves by using a lower number of $N_{m,s}$ (324 models for each subsample). At the same time, the numerical model of the real masonry aggregate was carried out and the fragility curves were obtained by varying the uncertain parameters as above indicated, for a total of 18 models, under the scheme reported in Fig. 12.

The comparison between the fragility curves of real and archetype masonry aggregates and the assessment of fragility curves of the real masonry aggregate within the minimum-maximum spindles are reported in Figs. 13 and 14, subdividing results in X and Y directions, respectively, and investigating each limit-state, and each failure mechanism (fragility for local mechanisms were evaluated with and without ring beams).

Looking in detail the obtained results, some aspects can be highlighted. First, the fragility curves evaluated on the real aggregate present the same trends of the archetype results in Figs. 8 and 9, with higher P_f in X direction (due to the openings) and lower P_f in Y directions. Observing the local fragility curves for all directions and considering or not the presence of the ring beam, the value of the dispersion β is extremely lower than the one derived for the archetypes, and this is mainly due to a slight variation of the uncertainties and, above all, to a variation of parameters do not strongly affecting the local behaviour (only the thickness of the walls). Instead, the important role of the varied mechanical parameters in global mechanisms provides a comparable dispersion between real and archetype aggregates for global fragility curves. Comparing the fragility curves of real and archetype buildings, in X direction results are in good agreement for all limit-states, especially for global mechanisms and local mechanisms without ring beam. Lower accuracy is observed for local mechanisms with ring beams, mainly caused by the obtained different dispersions (medians are not extremely different). Instead, in Y direction, a good agreement of results can be observed for local mechanisms (both for cases with and without ring beams), while for global mechanisms, the fragility of the real building tends to present a lower $P_{f,G}$, which suggests a certain conservativism in case of ultimate limit-states (i.e., LS and NC). Assessing the position of fragility curves for the real masonry aggregate within the minimum-maximum spindles, despite the inaccuracy in terms of dispersion, most of the curves presents medians within limits, which suggest good potentialities in prediction. Overall, META-FORMA-XL provides near good predictions for large-scale seismic analysis of masonry aggregates for both global and local mechanisms, and in some cases (e.g., LS and NC limit-states) it presents a certain conservativism. In the end, it is worth nothing that, looking at the mechanisms having the higher P_f according to Equation (20), the output of META-FORMA-XL perfectly fits with the fragility curve of the real masonry aggregate for all limit-states and analysis direction, which consists in the global behaviour for O limit-state and local behaviour without ring beam for the IO, LS, and NC limit-states.

5. Conclusions and further developments

The paper presents META-FORMA-XL, a procedure to estimate seismic fragility curves of masonry aggregates in historical centres through the combination of multi-source data and an automated typological-mechanical modelling of archetype buildings. In detail, META-FORMA-XL composes of six steps: (1) data collection of information about the existing building stock, by exploiting the output of interview-based approaches, such as CARTIS and data provided by freely available databases; (2) feature selection, subdividing data collected among deterministic and uncertain parameters; (3) automated generation of a huge number of archetype models, which account for different values of the selected parameters in likely ranges; (4) global analysis of archetype models, performed through pushover analysis; (5) local analysis of archetype models, performed through a nonlinear kinematic analysis and accounting or not for the presence of the ring beam; (6) derivation of fragility curves for both local and global mechanisms with respect to each limit-state and each analysis direction. After a detailed definition of the proposed procedure, META-FORMA-XL was applied to the case of Foggia, Puglia, Southern Italy, and on the row masonry aggregates in the historical centre. Results suggest how fragility curves vary with this aggregation form, as well as by considering the variation of the limit-states, the number of storeys, and the number of cells. Critical insights were provided also comparing global and local fragility curves, showing that as expected, local mechanisms (without ring beam) anticipate the failure obtained from global mechanisms. Still, the obtained results were validated on a real-life case study of masonry aggregate in the historical centre of Foggia, for which a near-full information about the geometrical features was available. The comparison, performed by evaluating a spindle of fragility curves, showed the capacity of the typological fragility curves produced by META-FORMA-XL to predict the seismic behaviour of real masonry aggregates.

In the end, several advantages can be highlighted from the proposed procedure. First, the possibility to identify the most likely collapse mechanism in this complex type of structures. Still, the approach preserves the main advantages of the original method, META-FORMA, which was aimed at generating and analysing typological models. As a matter of fact, the method is fast and allows to investigate a huge number of models in reasonable time, which is an important skill in a seismic large-scale analysis methodology. In addition, the method allows of accounting for all possible sources of uncertainty (i.e., geometrical, and mechanical features), which covers a paramount importance in a probabilistic-based investigation.

Close to the above advantages, some limitations of META-FORMA-XL should be highlighted, such as the current application to only row-masonry aggregates, which represent a small part of the possible aggregation shapes within historical centres. In fact, further developments will aim to extend the proposed concept to other aggregation forms, and to modify the META-FORMA-XL algorithm to introduce variability sources in the archetype models (e.g., different heights and different number of storeys among structural units). In addition, some modifications could be introduced in the generation of the models and the local and global analyses

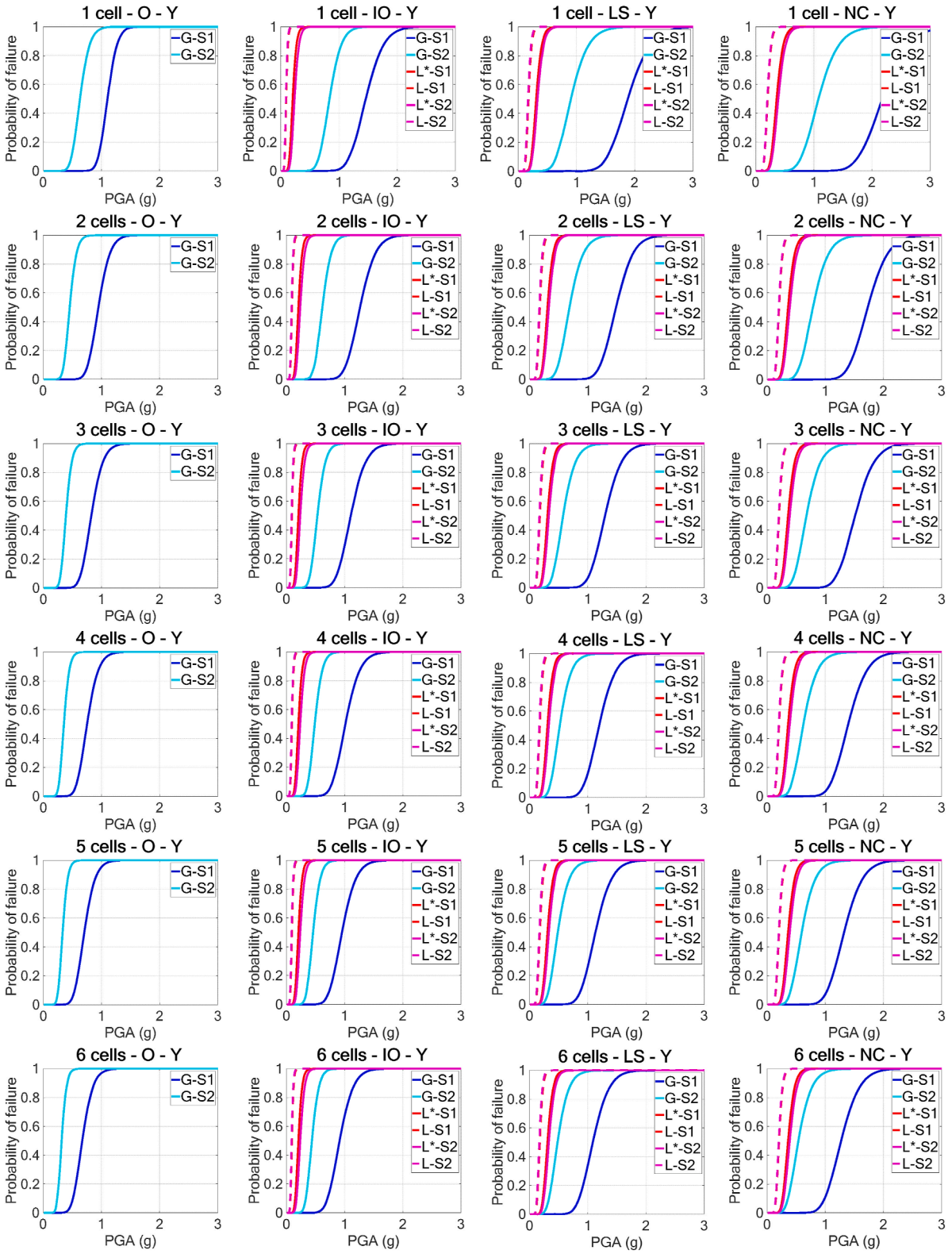

Fig. 9. Fragility curves in Y direction, accounting for local and global mechanisms (with and without ring beam), reported for each limit-state and varying the number of storeys and number of cells. G stands for global, L stands for local without ring beam, L* stands for local with ring beam. 1S and 2S indicate 1 storey and 2 storeys, respectively.

Fig. 10. Photo of the real row masonry aggregate used for purpose of validation.

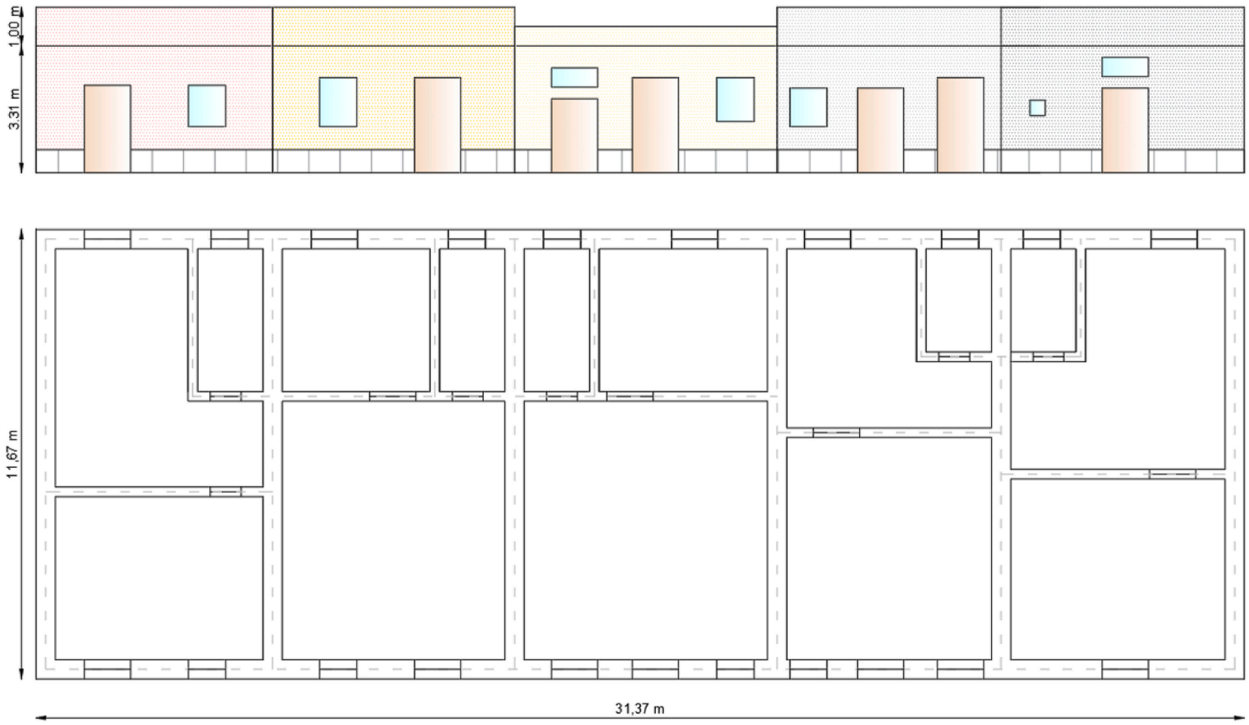

Fig. 11. Drawings of the surveyed row masonry aggregate. From the top to the bottom, elevation view of the buildings and planimetric distribution of masonry panels. Reported measures are expressed in meters (m) limited to the base area sides and height of the focused masonry aggregate.

Table 4
Definition of $P_{u,i}$ and related v_j to derive minimum and maximum fragility curves, for each limit-state, each direction, and each failure mechanism.

($P_{u,i}$ - v_j) Minimum fragility curves	($P_{u,i}$ - v_j) Maximum fragility curves
Percentage of openings at ground floor = 30%	Percentage of openings at ground floor = 20%
Percentage of openings at upper floors = 20%	Percentage of openings at upper floors = 10%
Thickness of walls = 0.25 m	Thickness of walls = 0.50 m
Type of masonry - $f_{c,m}$ = 2.041 MPa	Type of masonry - $f_{c,m}$ = 3.265 MPa
Type of masonry - $f_{v,m}$ = 0.102 MPa	Type of masonry - $f_{v,m}$ = 0.194 MPa

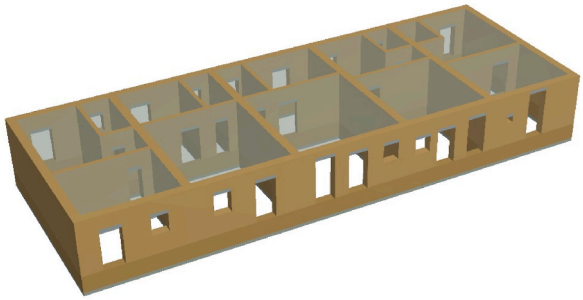

Fig. 12. Numerical model of the validation building, made in POR2000 [16].

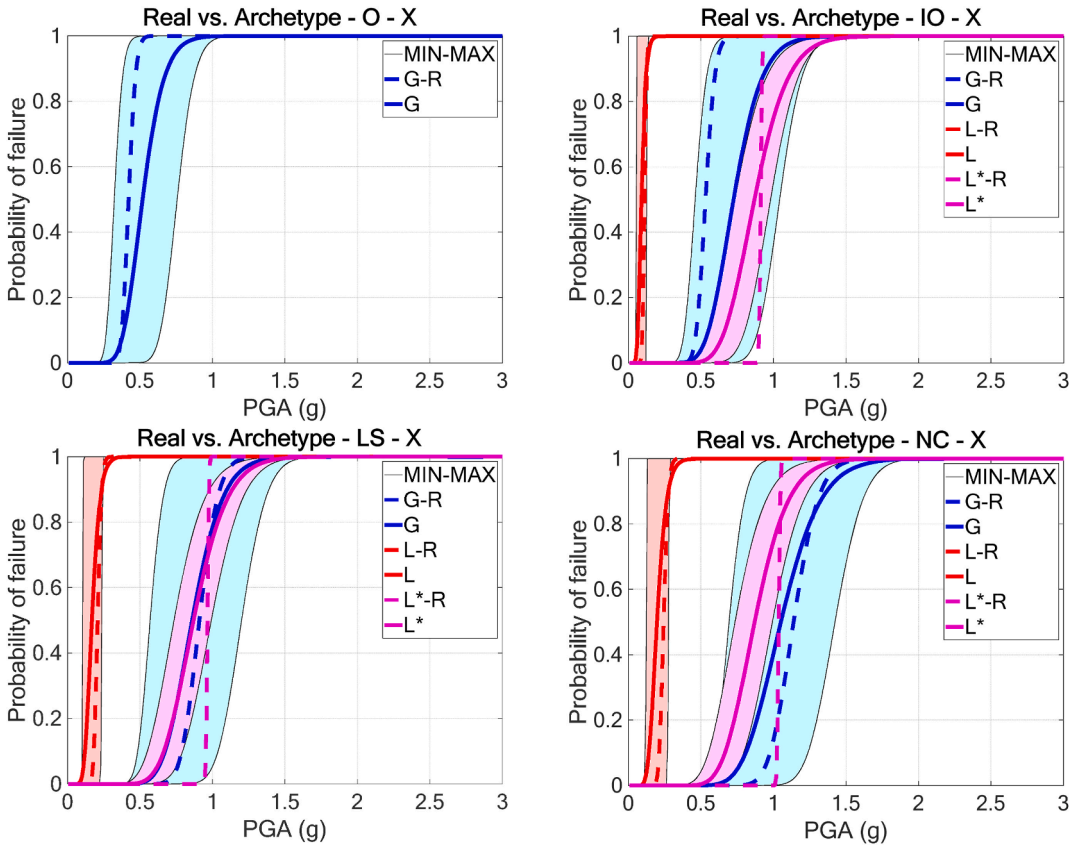

Fig. 13. Comparison of fragility curves between real (dashed line) and archetype (continuous line) buildings in X direction, accounting for local and global mechanisms (with and without ring beam), reported for each limit-state. G stands for global, L stands for local without ring beam, L* stands for local with ring beam, and R stands for real, respectively. Min-Max indicates the minimum and maximum fragilities for identifying the spindles curves for all failure mechanisms.

steps, in order to account for the possible presence of retrofit interventions, typical of the masonry aggregates in historical centres (e.g., steel ties, reinforced plaster).

Declaration of competing interest

The authors declare that they have no known competing financial interests or personal relationships that could have appeared to influence the work reported in this paper.

Data availability

Data will be made available on request.

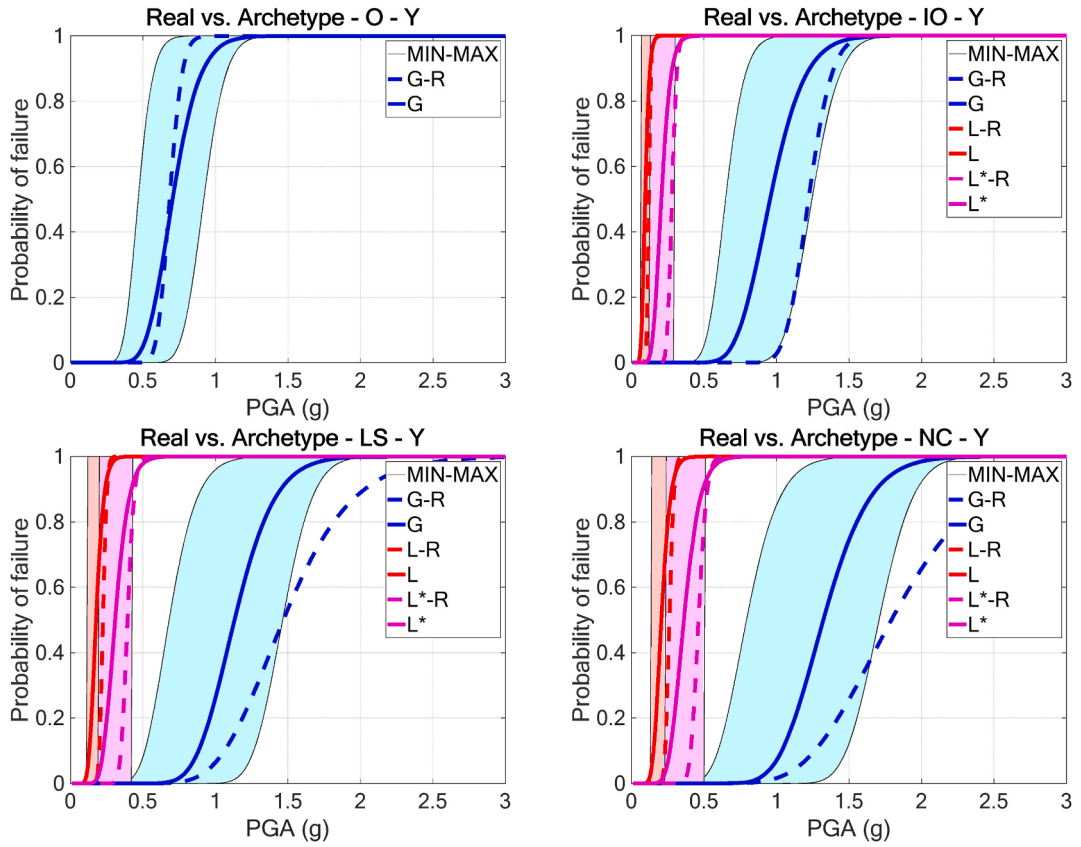

Fig. 14. Comparison of fragility curves between real (dashed line) and archetype (continuous line) buildings in Y direction, accounting for local and global mechanisms (with and without ring beam), reported for each limit-state. G stands for global, L stands for local without ring beam, L* stands for local with ring beam, and R stands for real, respectively. Min-Max indicates the minimum and maximum fragilities for identifying the spindles curves for all failure mechanisms.

Acknowledgement

This work was supported by the Italian Presidency of the Council of Minister, Civil Protection Department under the project CARTIS, WP2. Authors acknowledge the Newsoft company and Dr. Giuseppe Zagari from providing POR2000 and constant support.

References

[1] A. Rosti, C. Del Gaudio, M. Rota, P. Ricci, M. Di Ludovico, A. Penna, G.M. Verderame G M, Empirical fragility curves for Italian residential RC buildings, Bull. Earthq. Eng 19 (2021) 3165–3183, https://doi.org/10.1007/s10518-020-00971-4.

[2] A. Rosti, M. Rota, A. Penna, Empirical fragility curves for Italian URM buildings, Bull. Earthq. Eng. 19 (2021) 3057–3076, https://doi.org/10.1007/s10518-020-00845-9.

[3] S. Ruggieri, M. Calò, A. Cardellicchio G. Uva, Analytical-mechanical based framework for seismic overall fragility analysis of existing RC buildings in town compartments, Bull. Earthq. Eng. 20 (2022) 8179–8216, https://doi.org/10.1007/s10518-022-01516-7.

[4] V. Leggieri, S. Ruggieri, G. Zagari, G. Uva, Appraising seismic vulnerability of masonry aggregates through an automated mechanical-typological approach, Autom. ConStruct. 132 (2021) 103972, https://doi.org/10.1016/j.autcon.2021.103972.

[5] V. Silva, S. Akkar, J. Baker, P. Bazzurro, J.M. Castro, H. Crowley, M. Dolsek, C. Galasso, S. Lagomarsino, R. Monteiro, D. Perrone, K. Pitilakis, D. Vamvatsikos, Current challenges and future trends in analytical fragility and vulnerability modeling, Earthq. Spectra 35 (4) (2019) 1927–1952, https://doi.org/10.1193/042418EQS101O.

[6] L. Frassine, S. Giovinazzi, Basi di dati a confronto nell'analisi di vulnerabilità sismica dell'edilizia residenziale: un'applicazione per la città di Catania, XI Congresso Nazionale "L'ingegneria Sismica in Italia", Genova, 2004, p. 16. https://www.anidis.it/convegni-anidis/2004-genova/. (in Italian)).

[7] A. Sandoli, B. Calderoni, G.P. Lignola, A. Prota, Fragility curves for Italian URM buildings based on a hybrid method, Bull. Earthq. Eng. 19 (2021) 4979–5013, https://doi.org/10.1007/s10518-021-01155-4.

[8] P. Mouroux, E. Bertrand, M. Bour, B. Le Brun, S. Depinois, P. Masure, The European RISK-UE project: an advanced approach to earthquake risk scenarios, in: Proceedings of the 13th World Conference on Earthquake Engineering, 2004, p. 3329. https://www.iitk.ac.in/nicee/wcee/article/13_3329.pdf. (Accessed 12 May 2023).

[9] S. Brzev, C. Scawthorn, A.W. Charleson, L. Allen, M. Greene, K. Jaiswal, V. Silva, GEM Building Taxonomy Version 2.0, 2013, pp. 1–188 Technical Report. https://issuu.com/gem_wrld/docs/exp-mod-gem-building-taxonomy-20130. (Accessed 12 May 2023).

[10] V. Silva, S. Brzev, C. Scawthorn, C. Yepes, J. Dabbeek, H. Crowley, A building classification system for multi-hazard risk assessment, Int J Disaster Risk Sci 13 (2022) 161–177, https://doi.org/10.1007/s13753-022-00400-x.

[11] G. Zuccaro, M. Dolce, D. De Gregorio, E. Speranza, C. Moroni, La Scheda Cartis Per La Caratterizzazione Tipologico - Strutturale Dei Comparti Urbani Costituiti Da Edifici Ordinari. Valutazione dell'esposizione in analisi di rischio sismico, 34 Convegno Nazionale GNGTS, Trieste, 2015, pp. 281–287. http://www3.ogs.trieste.it/gngts/files/2015/S23/Riassunti/Zuccaro.pdf. (Accessed 12 May 2023).

[12] F.S. Liguori, S. Fiore, F. Perelli, D. De Gregorio, G. Zuccaro, A. Madeo A, Seismic vulnerability of masonry structures through a mechanical-based approach. ECCOMAS Congress, 2022. 8th European Congress on Computational Methods in Applied Sciences and Engineering. (2022) 5–9 https://doi.org/10.23967/

eccomas.2022.242, June 2022, Oslo, Norway.
[13] F.S. Liguori, S. Fiore, F.L. Perelli, D. De Gregorio, G. Zuccaro, A. Madeo, A mechanical-based seismic vulnerability assessment method with an application to masonry structures in Cosenza (Italy), Bull. Earthq. Eng. (2023).
[14] G. Brando, G. Cianchino, D. Rapone, E. Spacone, S. Biondi, A CARTIS-based method for the rapid seismic vulnerability assessment of minor Italian historical centres, Int. J. Disaster Risk Reduc. 63 (2021) 102478.
[15] V. Leggieri, G. Mastrodonato, G. Uva, GIS Multisource data for the seismic vulnerability assessment of buildings at the urban scale, Buildings 12 (5) (2022) 523, https://doi.org/10.3390/buildings12050523.
[16] MathWorks, MATLAB, Programming and Numeric Computing Platform, 2023. https://it.mathworks.com/products/matlab.html. (Accessed 12 May 2023).
[17] P.O.R.2000 Newsoft, Structural and Seismic Calculation and Analysis of Masonry Structures, 2023. https://www.newsoft-eng.it/software/por-2000. (in Italian)).
[18] P.B. Lourenço, J. Pina-Henriques, Validation of analytical and continuum numerical methods for estimating the compressive strength of masonry, Comp. & Struct. 84 (29–30) (2006) 1977–1989, https://doi.org/10.1016/j.compstruc.2006.08.009.
[19] G. Vasconcelos, P.B. Lourenço, Experimental characterization of stone masonry in shear and compression, Constr. Build. Mat. 23 (11) (2009) 3337–3345, https://doi.org/10.1016/j.conbuildmat.2009.06.045.
[20] S. Casolo, F. Pena, Rigid element model for in-plane dynamics of masonry walls considering hysteretic behaviour and damage, Earthq. Eng. Struct. Dynam. 36 (8) (2007) 1029–1048, https://doi.org/10.1002/eqe.670.
[21] L.F. Ramos, P.B. Lourenço, Modeling and vulnerability of historical city centers in seismic areas: a case study in Lisbon, Eng. Struct. 26 (9) (2004) 1295–1310, https://doi.org/10.1016/j.engstruct.2004.04.008.
[22] I. Senaldi, G. Magenes, A. Penna, Numerical investigations on the seismic response of masonry building aggregates, Adv. Mater. Res. (2010) 133–134. https://dx.doi.org/10.4028/www.scientific.net/AMR.133-134.715. 715–720.
[23] C. Fagundes, R. Bento, S. Cattari, On the seismic response of buildings in aggregate: analysis of a typical masonry building from Azores, Struct 10 (2017) 184–196, https://doi.org/10.1016/j.istruc.2016.09.010.
[24] M. Valente, G. Milani, E. Grande, A. Formisano, Historical masonry building aggregates: advanced numerical insight for an effective seismic assessment on two row housing compounds, Eng. Struct. 190 (2019) 360–379, https://doi.org/10.1016/j.engstruct.2019.04.025.
[25] C. Bernardini, R. Maio, S. Boschi, T.M. Ferreira, R. Vicente, A. Vignoli, The seismic performance-based assessment of a masonry building enclosed in aggregate in Faro (Portugal) by means of a new target structural unit approach, Eng. Struct. 191 (2019) 386–400, https://doi.org/10.1016/j.engstruct.2019.04.040.
[26] N. Grillanda, M. Valente, G. Milani, A. Chiozzi, A. Tralli, Advanced numerical strategies for seismic assessment of historical masonry aggregates, Eng. Struct. 212 (2020) 110441, https://doi.org/10.1016/j.engstruct.2020.110441.
[27] N. Grillanda, M. Valente, G. Milani, ANUB-aggregates: a fully automatic NURBS-based software for advanced local failure analyses of historical masonry aggregates, Bull. Earthq. Eng. 18 (8) (2020) 3935–3961, https://doi.org/10.1007/s10518-020-00848-6.
[28] L. Piegl, W. Tiller, The NURBS Book, Computer-Aided Design, Springer, Berlin, 1996, p. 646, https://doi.org/10.1016/0010-4485(96)86819-9. (Accessed 12 May 2023).
[29] M. Angiolilli, S. Lagomarsino, S. Cattari, S. Degli Abbati, Seismic fragility assessment of existing masonry buildings in aggregate, Eng. Struct. 247 (2021) 113218, https://doi.org/10.1016/j.engstruct.2021.113218.
[30] M. Angiolilli, A. Brunelli, S. Cattari, Fragility curves of masonry buildings in aggregate accounting for local mechanisms and site effects, Bull. Earthq. Eng. 21 (5) (2023) 2877–2919, https://doi.org/10.1007/s10518-023-01635-9.
[31] I. Senaldi, G. Guerrini, P. Comini, F. Graziotti, A. Penna, K. Beyer, G. Magenes, Experimental seismic performance of a half-scale stone masonry building aggregate, Bull. Earthq. Eng. 18 (2020) 609–643, https://doi.org/10.1007/s10518-019-00631-2.
[32] I. Tomić, A. Penna, M. DeJong, C. Butenweg, A.A. Correia, P.X. Candeias, K. Beyer, Shake-table testing of a stone masonry building aggregate: overview of blind prediction study, Bull. Earthq. Eng. (2023) 1–43, https://doi.org/10.1007/s10518-022-01582-x.
[33] A. Formisano, Theoretical and numerical seismic analysis of masonry building aggregates: case studies in San Pio Delle Camere (L'Aquila, Italy), J. Earthq. Eng. 21 (2) (2017) 227–245, https://doi.org/10.1080/13632469.2016.1172376.
[34] Ministero dei Beni e delle Attivit`a Culturali, Linee Guida per la valutazione e riduzione del rischio sismico del patrimonio culturale, 2010 (in Italian).
[35] R. Maio, R. Vicente, A. Formisano, H. Varum, R. Maio, Seismic vulnerability of building aggregates through hybrid and indirect assessment techniques, Bull. Earthq. Eng. 13 (10) (2015) 2995–3014 10.1007/s10518-015- 9747-9.
[36] G. Grünthal, European Macroseismic Scale 1998. Luxembourg: cahiers du Center Europ'een de Geodynamique et de Seismologie, Conseil de l'Europe, 99. http://media.gfz-potsdam.de/gfz/sec26/resources/documents/PDF/EMS-98_Origi nal_englisch.pdf, 1998.
[37] A. Formisano, G. Florio, R. Landolfo, F.M. Mazzolani, Numerical calibration of an easy method for seismic behaviour assessment on large scale of masonry building aggregates, Adv. Eng. Software (2015) 116–138 10.1016/j. advengsoft.2014.09.013.
[38] G. Chiumiento, A. Formisano, Simplified and refined analyses for seismic investigation of historical masonry clusters: comparison of results and influence of the structural units position, Front. in Built Env. (2019) 5–84, https://doi.org/10.3389/fbuil.2019.00084.
[39] N. Chieffo, A. Formisano, Comparative seismic assessment methods for masonry building aggregates: a case study, Front. in Built Env. (2019) 5–123, https://doi.org/10.3389/fbuil.2019.00123.
[40] A. Bernardini, R. Gori, C. Modena, M.R. Valluzzi, G. Beninca, E. Barbetta, A. Bernardini, Vulnus Vb 4.0: Procedura Automatica per Analisi di Vulnerabilità Sismica di Edifici in Muratura, 2009. http://hdl.handle.net/11577/3150148. (In Italian).
[41] A. Greco, G. Lombardo, B. Panto, A. Fama, Seismic vulnerability of historical masonry aggregate buildings in oriental Sicily, Int. J. Architect. Herit. 14 (4) (2020) 517–540, https://doi.org/10.1080/15583058.2018.1553075.
[42] G. Cocco, A. D'Aloisio, E. Spacone, G. Brando, Seismic vulnerability of buildings in historic centers: from the "urban" to the "aggregate" scale, Front. in Built Env (2019) 5–78, https://doi.org/10.3389/fbuil.2019.00078.
[43] G. Brando, G. De Matteis, E. Spacone, Predictive model for the seismic vulnerability assessment of small historic centres: application to the inner Abruzzi Region in Italy, Eng. Struct. 153 (2017) 81–96, https://doi.org/10.1016/j.engstruct.2017.10.013.
[44] A. Formisano, N. Chieffo, P.G. Asteris, P.B. Lourenço, Seismic risk scenario for the historical centre of castelpoto in Southern Italy, Earthq. Eng. Struct. Dynam. (2023), https://doi.org/10.1002/eqe.3887.
[45] S. Ruggieri, A. Cardellicchio, V. Leggieri, G. Uva, Machine-learning based vulnerability analysis of existing buildings, Autom. ConStruct. 132 (2021) 103936, https://doi.org/10.1016/j.autcon.2021.103936.
[46] A. Cardellicchio, S. Ruggieri, V. Leggieri, G. Uva, V.U.L.M.A. View, Data set for training a machine-learning tool for a fast vulnerability analysis of existing buildings, Data 7 (1) (2022) 4, https://doi.org/10.3390/data7010004.
[47] Ministero delle Infrastrutture e dei Trasporti, Aggiornamento delle "Norme tecniche per le costruzioni" (in Italian), 2018. https://www.gazzettaufficiale.it/eli/gu/20 18/02/20/42/so/8/sg/pdf.
[48] Ministero delle Infrastrutture e dei Trasporti, Circolare 21 gennaio 2019 n.7 "Istruzioni per l'applicazione dell'«Aggiornamento delle 'Norme tecniche per le costruzioni'» di cui al decreto ministeriale 17 gennaio 2018", 2019 (in Italian). https://www.gazzettaufficiale.it/eli/id/2019/02/11/19A00855/sg.
[49] C.G. Jung, The Archetypes and the Collective Unconscious, Routledge, 2014.
[50] M. Tomazevic, The computer program POR, in: Report ZRMK, in Slovenian), Ljubljana, 1978. https://scholar.google.com/. (Accessed 12 May 2023).
[51] A. Bilotta, R. Casciaro, Assumed stress formulation of high order quadrilateral elements with an improved in-plane bending behaviour, Comput. Methods Appl. Mech. Eng. 191 (15–16) (2002) 1523–1540, https://doi.org/10.1016/S0045-7825(01)00334-6.
[52] S. Brasile, R. Casciaro, G. Formica, Finite element formulation for nonlinear analysis of masonry walls, Comput. Struct. 88 (3–4) (2010) 135–143, https://doi.org/10.1016/j.compstruc.2009.08.006.
[53] C. Casapulla, L.U. Argiento, A. Maione, E. Speranza, Upgraded formulations for the onset of local mechanisms in multi-storey masonry buildings using limit analysis, Struct 31 (2021) 380–394, https://doi.org/10.1016/j.istruc.2020.11.083.
[54] S. Lagomarsino, Seismic assessment of rocking masonry structures, Bull. Earthq. Eng. 13 (2015) 97–128, https://doi.org/10.1007/s10518-014-9609-x.

[55] P. Fajfar, Capacity spectrum method based on inelastic demand spectra, Earthq. Eng. Struct. Dynam. 28 (9) (1999) 979–993 https://doi.org/10.1002/(SICI)1096-9845, 199909)28:9<979::AID-EQE850>3.0.CO;2-1.
[56] F. Jalayer, C.A. Cornell, Alternative non-linear demand estimation methods for probability-based seismic assessments, Earthq. Eng. Struct. Dynam. 38 (8) (2009) 951–972, https://doi.org/10.1002/eqe.876.
[57] J.W. Baker, Efficient analytical fragility function fitting using dynamic structural analysis, Earthq. Spectra 31 (1) (2015) 579–599 10.1193/021113EQS0 25M.
[58] ISTAT, 15◦ Censimento generale della popolazione e delle abitazioni. https://istat. it/, 9th October 2011 (accessed on May 12, 2023, in Italian).
[59] C. Tosto, V. Leggieri, S. Ruggieri, G. Uva, Investigation of architectural typological parameters influencing seismic vulnerability of masonry buildings in historical centres: the case of Puglia, Procedia Struct. Integr. 44 (2023) 2036–2043, https://doi.org/10.1016/j.prostr.2023.01.260.